Additional Thesis (AES4011-10)
Modelling pavement evaporative cooling to mitigate heat wave

Student: Guoshiuan Lin
Student Number: 5283000
Study program: MSc Applied earth Science – Environmental Engineering track
Supervisors:
Dr. Alejandro Figueroa, Swiss Federal Institute of Aquatic Science and Technology
Dr. Marie-claire ten Veldhuis, Delft University of Technology
Dr. Stephan de Roode, Delft University of Technology

Abstract

As the intensity and frequency of urban heat wave increases in Europe, evaporative cooling from watering pavements has been considered as a promising strategy to regulate urban temperature. The aim of this research is to include evaporative cooling modelling and enhance the surface temperature model SURF-TEMP, which is in development at the Swiss Federal Institute of Aquatic Science and Technology (Eawag), to predict the optimal use of water resources towards mitigating urban heat. In order to test various evaporation models found in literature, we first developed a simple Python model to evaluate ten evaporation models. Differences among the simulated evaporative heat fluxes and surface temperature reduction can be around two folds under the same simulation condition for different evaporative cooling models. Besides the evaporation models, three equations to obtain the convective heat transfer coefficient were tested. We tested their uncertainties and determined the equation that provides the most neutral estimation on convective heat transfer coefficient. We proceeded to conduct various simulations to understand the sensitivity of these evaporation models with respect to four factors (wind speed, relative humidity of air, initial surface temperature, and initial water height). These factors influence the evaporative cooling efficiency and therefore the optimal watering rate. Two evaporative models that represent the higher and lower limit of the simulated evaporative heat flux are incorporated into SURF-TEMP. Results show that the model that estimates the highest evaporative heat flux is in good agreement with the lab measurement published by (Parison et al.,2020) when watering rate is equal or above 1 mm per hour. When watering rate falls below 0.75 mm per hour, the models studied underestimate the evaporative heat flux and surface temperature reduction. Discrepancies during low watering rate are caused by the absence of modelling of water conduction and infiltration with the pavement, non-linear relation of evaporation rate with vapor pressure difference, and the inherent error between simulation and experimental results even under dry condition.

Highlight

- Development of a Python code that simulates ten evaporative cooling models available in the literature. Two of them are integrated into SURF-TEMP, a FORTRAN code that estimates surface temperature.
- The influence of wind speed, surface temperature, and air relative humidity on evaporative cooling is studied. Wind speed is the variable that has the largest effect on modelling evaporative cooling.
- Cooling efficiency and therefore optimal watering rate depends on the evaporation models used and weather conditions.
- SURF-TEMP shows good agreement with evaporative heat flux and surface temperature measurements for watering rates higher than 0.75 mm/hr, however for watering rates lower than 0.75 mm/hr the model yields reduce its accuracy.

Nomenclature

B: Thermal expansion coefficient [$1/k$]
Cp,air: Specific heat capacity of air, 1004 [$J/kg \cdot K$]
Cp,p: Specific heat capacity of pavement, 750 [$J/kg \cdot K$]
Cp,w: Specific heat capacity of water, 4200 [$J/kg \cdot K$]
d: Length of the water pond [m]
ds: Depth of the pavement's surface, 0.1 [m]
dx: Depth of the pavement, 0.32 [m]
D: Diffusion coefficient of water vapor to the air [-]
E: Evaporation rate [mm/hr]
g: Gravity, 9.8 [m/s^2]
h: Convective heat transfer coefficient [-]
hw: Water height [m]
k: Thermal conductivity of pavement, 1.38 [$W/m \cdot K$]
kw: thermal conductivity of water [$W/m \cdot K$]
L: Longwave radiation [W/m^2]
L: Characteristic length [m]
L: Longwave radiation [W/m^2]
Le: Lewis number [-]
Lv: Vaporization heat of water [*J/kg*]
Nu: Nusselt number [-]
Psat: Saturation vapor pressure [*Pa*]
P_0: Atmospheric pressure, 101300 [*Pa*]
Qe: Evaporative cooling flux [W/m^2]
Qcond: Conductive heat flux in the pavement [W/m^2]
Qconv: Convective heat flux between surface and the air [W/m^2]
Qconv, sw: Convective heat flux between pavement's surface and water [W/m^2]
R: Net radiation at the surface, 750 [W/m^2]
Ra: Rayleigh number [-]
RH: Relative humidity [-]
r_s: Bulk evaporative resistance, 200 [*s/m*]
S: Shortwave radiation [W/m^2]
Sh: Sherwood number [-]
SEB: Surface energy balance [W/m^2]
T_0: Temperature of air, 308 [*K*]
Ts: Temperature of pavement's surface [*K*]
Tb: Temperature of pavement's bottom, 303 [*K*]
Tf: Film temperature [*K*]
Tw: Temperature of water [*K*]

v: Wind speed, 1 [m/s]

WEB: Water energy balance [W/m^2]

α_{water}:Albedo of water to shortwave radiation, 0.06 [-]

$\alpha_{pavement}$:Albedo of pavement to shortwave radiation, 0.08 [-]

$\varepsilon_{wet\ pavement}$:Emissivity of wet pavement, 0.98 [-]

$\varepsilon_{pavement}$:Emissivity of pavement, 0.99 [-]

β: average mass transfer coefficient [-]

ρ_{air}: Density of air, 1.225 [kg/m^3]

ρ_p: Density of pavement, 2150 [kg/m^3]

ρ_w: Density of water, 1000 [kg/m^3]

μ: Viscosity of water, 10^{-6} [$Pa{\cdot}sec$]

1. Introduction

There is growing evidence that climate change effects will lead to a higher frequency of heat waves and extreme rainfall events (King & Karoly, 2017; Fowler & Kilsby, 2003; Min, et al., 2011). In particular, European cities will experience more intense, more frequent, and longer-lasting heat waves during summer periods in the second half of the 21st century compared to previous decades (Anon., 2018; Meehl & Tebaldi, 2004).

As the frequency of extreme heat waves in Europe increases, developing an efficient strategy to mitigate high temperature is crucial. Improving thermal comfort (i.e., the "satisfaction" of the human body in a given thermal environment) indexes during heat wave events will benefit all member of the society and increase livability. Heat waves have a negative impact on public health, people's well-being (Lafortezza, et al., 2009), energy power consumption and urban infrastructure. An epidemiological study about heat related mortality in different settings around the world suggests that the risk of mortality increases by between 1% and 3% per 1°C change in high temperature (Hajat & Kosatky, 2010). The high electricity demand during the unprecedented Northwest U.S. heat wave in June 2021 caused consecutive blackouts in Washington state (Johnson & Geranios, 2021) . In addition, studies show that heat wave event presents a major threat to increased heat related damage on infrastructure (McEvoy, et al., 2012) and reduction of economic productivity (Xia, et al., 2018).

Due to the increase of heatwaves events and extreme rainfall, the development of clever water management strategies that alleviate their effects are critical to improve livability indicators in cities. Some recent studies proposed to use evaporative cooling methods to mitigate heat waves related problems, such as the urban heat phenomena. Mitigation measures such as pavement watering has been studied as an emergency cooling tool in districts of Paris and Lyon (Hendel, et al., 2016). Understanding the physical processes of pavement cooling on different surface materials and the built environment is essential for the development of effective cooling strategies. Therefore, several studies have been dedicated to analyzing and model the thermodynamic processes involved during pavement watering (Azam, et al., 2018; Hendel, et al., 2015; Parison, et al., 2020). However, most of these models are based on experimental data, and they are not generally applicable since they reproduce only specific thermal and physical conditions.

Eawag, The Swiss Federal Institute of Aquatic Science and Technology initiated the StormHeatX project with the goal of studying the impact of harvesting stormwater to cool down cities during heatwaves.

Recent efforts led to the creation of SURFT-TEMP, a 1-D numerical tool that simulates surface temperatures based on environmental variables, including air temperature and humidity, solar radiation, wind velocity, and pavement material properties. However, like many other existing microclimate models, the tool lacks sufficient validation. In addition, a model for evaporative cooling is not integrated into the present 1-D numerical tool yet.

This research aims to further develop the SURF-TEMP model in order to predict urban surface temperatures during evaporative cooling practices. Furthermore, the obtained model will be validated with real-world data, and it is expected that will help to accurately predict and optimize the impact of pavement watering practices on urban surfaces.

By coupling the SURF-TEMP with existing Computational Fluid Dynamics (CFD) models, temperatures in a street canyon or city districts could be simulated with high level of detail and allowing for thermal comfort calculations. The results of the research will contribute to a paradigm shift from the concept of draining stormwater from urban areas to harvesting stormwater co-benefits, such as cooling, harvesting energy, and increasing urban biodiversity.

The report is structured as follows:

- chapter 2 details the material and methods, including the thermodynamic and structure of the Python model and the SURF-TEMP model,
- chapter 3 presents the uncertainty (evaporation models and convective heat transfer coefficients) and sensitivity analysis (wind speeds, humidity, surface temperature) of the Python code and results of optimal watering rate by the Python model,
- chapter 4 shows the validation of Python model and SUR-TEMP with the existent theoretical models, lab measurement, and field observation on evaporative cooling,
- chapter 5 discusses two main challenges in the research: the heat transfer model between pavement surface and water film, and disagreement of simulation and lab observations.

2. Material and Methods

The development of the simulation model consists of three steps. First, a Python code is built with the goal of performing uncertainty and sensitivity analysis of several evaporation models. Second, selected evaporation models will be integrated into SURF-TEMP. The main difference between the two simulation tools is that the first one is written in Python and surface temperatures are calculated using an explicit time discretization; while the second one is programmed in Fortran and the temperature is implicitly computed using the Crank-Nicolson method. Third, we will proceed to validate the previously mentioned tools with field and laboratory measurements available in the literature.

2.1 Pavement structure

As the goal is to focus on the understanding of the pavement cooling from water evaporation, the Python model is composed of only three components: air, water film, and pavement. The air temperature is fixed at 308 K. The initial sprinkled water is at the same temperature as the air temperature at 308 K. Initial temperature of the pavement's surface is 323 K, which is a common value for urban surface during heat wave. The surface temperature, wind speed, atmospheric relative humidity, and added water height can be adjusted as desired. The model structure is shown in Figure 1.

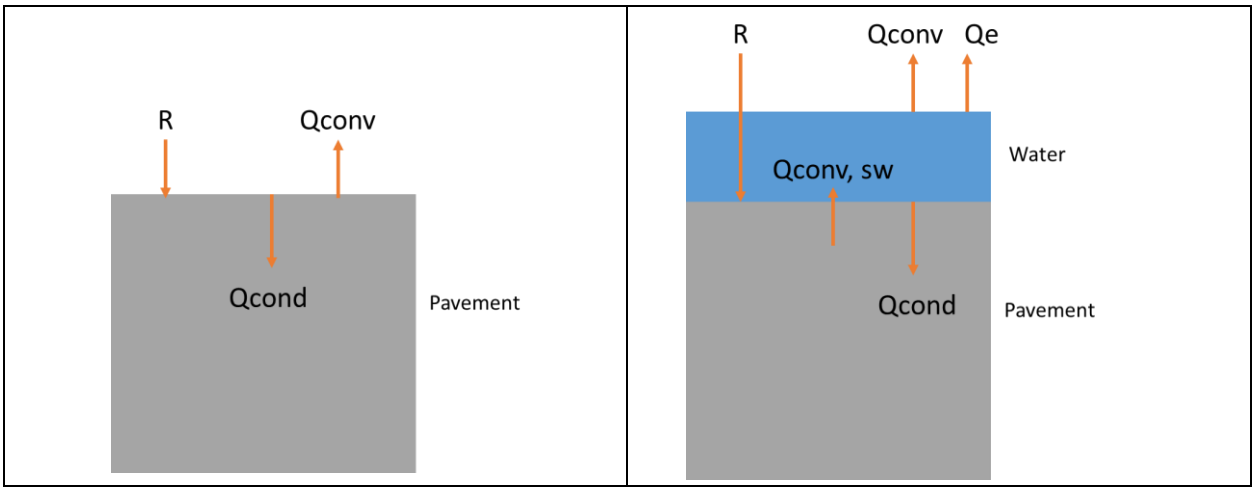

Figure 1. Structures of the pavement model under dry (left) and wet conditions (right)

To validate the Python model with the experimental results, the thermal properties of the pavement are defined according to (Parison, et al., 2020). The pavement is composed of a single material with a surface area of 1 m^2 and depth of 32 cm. Its density, thermal conductivity, and specific heat capacity are 2150 kg/m^3, 1.38 $W/m \cdot K$, and 750 $J/kg \cdot K$ respectively. The temperature at the bottom of the pavement is assumed to be constant at 298K. The top 10 cm_of the pavement is considered as the pavement's surface. Its variation in temperature is simulated to understand the effect of evaporative cooling.

In the SURF-TEMP, the pavement is composed of three layers of different materials as the asphalt road described in (Parison, et al., 2020). The structure of the pavement is shown in Figure 2. The thermal properties of each layer are listed in Table 1.

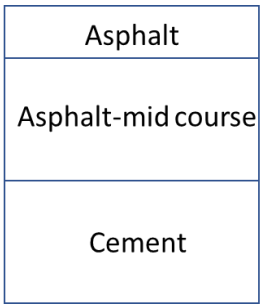

Figure 2. Pavement structure in the SURF-TEMP model

Table 1. Thermal properties of each material layer

	Asphalt	Asphalt mod-course	Cement
Thermal conductivity, k $[W/m \cdot K]$	1.77	1.63	1.18
Density, ρ, $[kg/m^3]$	2305	2360	1946
Heat capacity, C_p $[J/kg \cdot K]$	725	806	714

2.2 Energy balance under dry condition

Three major heat fluxes affect the energy balance at the pavement's surface. First, radiation at the surface. The net radiation is controlled by shortwave and longwave radiation. This can be modeled by the methods proposed in (Parison, et al., 2020). The net radiation at the surface is

$$R_{dry} = \left(1 - \alpha_{pavement}\right)S + \varepsilon_{pavement}(L - T_s^4)$$

Eq (1)

Second, the conductive heat flux (Q_{cond}) from the surface (higher temperature) to the bottom of the pavement (constant, lower temperature). It is modelled by the Fourier's law, as shown in Eq (2) in which dx is the depth of the pavement.

$$Q_{cond} = k\frac{dT}{dx} = k\frac{T_s - T_b}{dx}$$

Eq (2)

Third, the convective heat flux between the pavement and air (Q_{conv}). It is modelled by the Newton's law of cooling.

$$Q_{conv} = h(T_s - T_0)$$

Eq (3)

In most models presented in the literature, the convective heat transfer coefficient between water and air (h) is parameterized as a function of wind(v) in the form of Eq (4). In our work, three linear functions are tested, as summarized in Table 2.

$$h = a \times v + b$$

Eq (4)

Table 2. Common equations for the convective heat transfer coefficient for low wind speed conditions

Convective heat transfer coefficient (h)	Reference	Conditions
h=5.62 + 3.9 v	(ASHRAE, 1993)	Wind tunnel measurement, plate, parallel flow, wind speed < 5 *m/s*, smooth surface. (Bentz, 2000) has similar results for concrete surface: 5.6 + 4 v
h=4.2 + 3.5 v	(Palyvos, 2008)	Wind speed 0 ~ 4.5 *m/s*. Leeward surface
h=6.15 + 4.18 v	(Kusaka, et al., 2001)	Wind speed < 5 *m/s*. building roof, building wall, and road

The sum of the radiative, conductive, the convective heat flux is also referred to surface energy balance (SEB) in this report. Therefore, the SEB under dry condition is

$$Surface\ Energy\ Balance\ (SEB) = R - Q_{conv} - Q_{cond}$$

Eq (5)

Overall, with the SEB and the thermal properties of the pavement, temperature of pavement can be simulated by using an explicit in time discretization method. The surface temperature is modelled by Eq (6).

$$T_s^{t+1} = \frac{dt}{d_x \rho_p C_p}(SEB) + T_s^t$$

Eq (6)

Were d_x, ρ_p, C_p are the depth (m), density (kg/m^3) and specific heat capacity ($J/kg \cdot K$) of the pavement surface respectively.

2.3 Energy balance under wet condition

The energy balance changes when there is water above the pavement. The radiation and the convective heat flux between surface and the air change due to the presence of water. Besides, two additional fluxes appear in the system. They are the latent heat flux from water evaporation and the convective heat flux between pavement and water. When the surface is wet, the albedo of water should be considered instead of the pavement. The emissivity of dry and wet pavement is also different. Therefore, the net radiation becomes

$$R_{wet} = (1 - \alpha_{water})S + \varepsilon_{wet\ pavement}(L - T_s^4)$$

Eq (7)

We assume that the thin water film (< 2mm) is transparent to radiation, therefore it enters directly into the pavement. Convection with air also changes because air is in contact with the water, not the pavement. So Eq (3) becomes

$$Q_{conv} = h(T_w - T_0)$$

Eq (8)

The third relevant heat flux is the convective heat flux between the pavement and the water film. Most of the existent pavement cooling models assume that the temperature of the water film and pavement surface are the same ((Parison, et al., 2020) & (Hendel, et al., 2015)), so the convective flux ($Q_{conv,sw}$) is zero. Yet, we chose to model this flux especially because the temperature between water and pavement surface can be different when water lies on top of the pavement. As water on the pavement evaporates, the flux ($Q_{conv,sw}$) transfers the latent cooling from the water film to the pavement and reduce its temperature. Therefore, it's a decisive flux in our model. The heat flux between pavement and water film ($Q_{conv,sw}$) is modelled making use of the equation that defines free convective heat flow on the upper surface of hot plate in (Bergman, et al., 2011).

The convective heat flux between pavement and water is driven by their temperature difference and the convective heat transfer coefficient (h_{sw}) according to Eq (9).

$$Q_{conv,sw} = h_{sw}(T_s - T_w)$$

Eq (9)

The convective heat transfer coefficient (h_{sw}) can be computed by Eq (10).

$$h_{sw} = k_w \frac{Nu}{L}$$

Eq (10)

The thermal properties of the water should be assessed by the film temperature (T_f) which is the average temperature between pavement surface and water.

$$T_f = \frac{T_s + T_w}{2}$$

Eq (11)

K_w is the thermal conductivity of water $\left(\frac{W}{m} \cdot K\right)$ and it computed by the regressed equation defined by (Reid, et al., 1987).

$$k_w = -6.369 \times 10^{-6} {T_f}^2 + 5.254 \times 10^{-3} T_f - 0.3838$$

Eq (12)

Following the guidelines from (Bergman, et al., 2011), the characteristic length is calculated by the area divided by the perimeter of the water pond.

$$L = \frac{Area}{Perimeter}$$

Eq (13)

For instance, for a square water surface of 1 m^2, L is therefore 0.25 m. Depending on the Rayleigh number, the recommended average Nusselt number in (Bergman, et al., 2011) are

$$Nu = 0.54 Ra^{0.25} \ \ if \ Ra < 10^7$$
$$Nu = 0.15 Ra^{\frac{1}{3}} \ \ if \ Ra \geq 10^7$$

Eq (14)

With Rayleigh number (Ra) defined by Eq (15).

$$R_a = \frac{g B L^3 \rho_w C_{p,w} (T_s - T_f)}{\mu k_w}$$

Eq (15)

The thermal expansion coefficient (B) required by Eq. (6) is computed by Eq (16) (Irvine Jr & Duignan, 1985).

$$B = -(a0 + a1 \times T_f + a2 \times T_f^2 + a3 \times T_f^3 + a4 \times T_f^4)$$
$$a0 = 6.12904369 \times 10^{-5}$$
$$a1 = -1.67585971 \times 10^{-5}$$
$$a2 = 1.95633218 \times 10^{-7}$$
$$a3 = -1.62858017 \times 10^{-9}$$
$$a4 = 5.39048385 \times 10^{-12}$$

Eq (16)

With this calculation above, the convective heat transfer between water and pavement surface is obtained.

The main flux we aim to analyze in the work is the evaporative cooling flux (Qe). To identify the optimal model in accordance with lab and field data, ten models from literature are reproduced and compared. The models are summarized in Table 3. Descriptions of the ten selected evaporative models can be found

in the Appendix. All these models show that evaporative cooling is driven by two mechanisms. First, forced convection is strongly dependent by wind characteristics which is modelled into the convective heat transfer coefficient (h). Second, latent heat transfer which is driven by vapor pressure (or vapor density or temperature) gradient between water surface and the air. Saturation vapor pressure in the simulation is modeled by Eq (17) in which saturation vapor pressure (P_{sat}) is in the unit of Pa and temperature (T) is in the unit of °C.

$$P_{sat} = 611.2\exp\left(\frac{16.67T}{243.5+T}\right)$$

Eq (17)

Although the main structures of these evaporation models are similar, they show discrepancy in the constants, parameterization of the forced convection, and how their driving forces for evaporation are calculated.

Table 3. Descriptions of the ten selected evaporative models

	Reference	Evaporative Cooling Model (W/m2)	Comment
1	(Parison, et al., 2020)	$Q_e = 0.622\frac{L_v h}{C_{p,air}P_0}T_w\left(\frac{P_{sat}(T_w)}{T_w} - \frac{RH \times P_{sat}(T_0)}{T_0}\right)$	Theory
2	(Azam, et al., 2018)	$Q_e = 0.622\frac{L_v h}{C_{p,air}}\left(\frac{P_{sat}(T_w)}{P_0 - 0.378P_{sat}(T_w)} - \frac{RH \times P_{sat}(T_0)}{P_0 - RH \times 0.378P_{sat}(T_0)}\right)$	Theory
3	(Bergman, et al., 2011)	$Q_e = \frac{L_v * h * 0.018}{8.314 * \rho_{air} * C_{p,air}} \times \left(\frac{P_{sat}(T_w)}{T_w} - \frac{RH \times P_{sat}(T_0)}{T_0}\right)$	Theory. Le is assumed to be 1
4	(Pagliarini & Rainieri, 2011)	$Q_e = 0.622\frac{L_v h}{C_{p,air}P_0}\frac{T_w + T_0}{2}\left(\frac{P_{sat}(T_w)}{T_w} - \frac{RH \times P_{sat}(T_0)}{T_0}\right)$	Theory
5	(Raimundo, et al., 2014)	$Q_e = 10^{-9}L_v(37.17 + 32.19v)(P_{sat}(T_w) - RH \times P_{sat}(T_0))$	Experiment. Wind tunnel measurement
6	(Tang & Etzion, 2004)	$Q_e = (0.2253 + 0.24644v)(P_{sat}(T_w) - RH \times P_{sat}(T_0))^{0.82}$	Experiment. Evaporation from outdoor pond
7	(Tiwari, et al., 1982)	$Q_e = 0.013h(P_{sat}(T_w) - RH \times P_{sat}(T_0))$	Experiment. Evaporation from roof
8	(Herb, et al., 2008)	$Q_e = 0.0015 \times \frac{0.018}{8.314}\rho_a L_v(v + (T_w - T_0)^{0.33})\left(\frac{P_{sat}(T_w)}{T_w} - \frac{RH \times P_{sat}(T_0)}{T_0}\right)$	Theoretical model calibrated with field measurement.
9	(Qin & Hiller, 2016)	$Q_e = \frac{L_v}{r_a + r_s}(\rho_{air}(T_0) - \rho_{air,sat}(T_w))$	Evaporation from pervious surface
10	(Min & Tang, 2015)	$Q_e = L_v\frac{h}{c_{p,a}L_e^{\frac{2}{3}}}(w(T_w) - w(T_0))$	Theory

With the evaporative cooling models and the equations of the three other heat fluxes above, energy balance of the water film (WEB) is calculated according to Eq (18).

$$Water\ Energy\ Balance\ (WEB): Q_{conv,sw} - Q_{conv} - Q_e$$

Eq (18)

Temperature of the water film can be simulated by the same explicit method with the thermal properties of water, as shown in Eq (19).

$$T_w^{t+1} = \frac{dt}{h_w \rho_w C_w}(WEB) + T_w^t$$

Eq (19)

The surface energy balance under wet condition becomes

$$Surface\ Energy\ Balance\ (SEB) = R - Q_{conv,sw} - Q_{cond}$$

Eq (20)

2.4 Heat flux dynamic (Python code)

With the aim of simulating surface temperatures in presence of a film of water, a zero-dimension python code is developed and tested. The code is capable of simulating heat fluxes and temperature of pavement surface during evaporative cooling practices. The dynamic of the model is shown in Figure 3. To start the simulation, the model first detects if there's water on the pavement. If the water height is above 0.01 mm, the water energy balance (WEB) and surface energy balance (SEB) are calculated based on Eq (18) and Eq (20) with the heat fluxes at the time step t. Proceeding with the WEB and SEB, the temperature of water and pavement's surface at time step t+1 are calculated by Eq (19) and Eq (6). Meanwhile, the water height at time step t+1 is updated by the previous water height minus the height of the evaporated water during the time step. With the updated water height at each step, the model proceeds until the end of simulation.

If the water height at the time step t is lower than 0.01 mm, the surface is regarded as dry (no water). The model then enters the dry model. Its SEB is described in Eq (5). The surface temperature then changes according to the new SEB using Eq (6). The water height in the next time step is assumed to be reduced to zero. Because there is no more water added, the model keeps running in the dry model until the end of the simulation. The Python model does not allow for water to be sprayed to the pavement periodically.

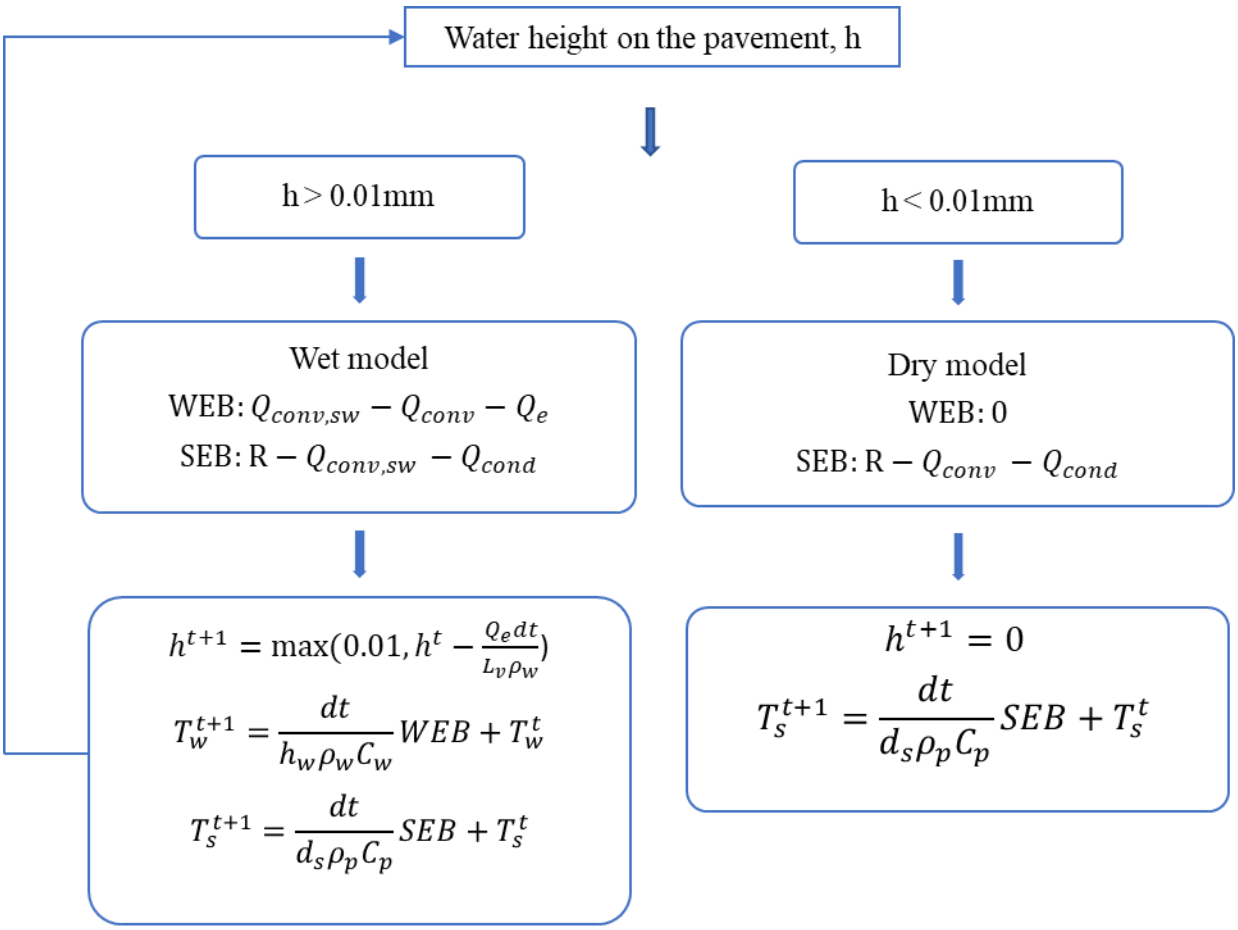

Figure 3. Flow chart of the thermal dynamics in the Python model

2.5 Heat flux dynamic (SURF-TEMP)

Selected evaporative cooling models are then integrated into the SURFT-TEMP code. This code is under development and is designed to estimate temperature across multiple impervious materials. It discretizes the 1D heat transfer equation using a hybrid finite difference/finite volume method to conserve fluxes at the interfaces between materials and an implicit scheme for time integration. Therefore, the modelled temperature at time step *t+1* takes the variables at both time steps *t* and *t+1* into account and producing a modelling tool that is more stable numerically. The implicit method is shown in Eq (21). A factor θ in the numerators decides the weighting between time steps *t* and *t+1*. We chose θ = 0.5, the so-called Crank-Nicolson method. t denotes the time step and i denotes the spatial step (depth).

$$\frac{T_i^{t+1} - T_i^t}{\Delta t} = \frac{\alpha\theta(T_{i-1}^{t+1} - 2T_i^{t+1} + T_{i+1}^{t+1})}{\Delta x^2} + \frac{\alpha(1-\theta)(T_{i-1}^{t} - 2T_i^{t} + T_{i+1}^{t})}{\Delta x^2}$$

Eq (21)

SURF-TEMP allows for the definition of Neumann, Dirichlet or Robin boundary conditions (BC) at the top (interface between the impervious materials and atmosphere) and bottom of the system (interface between the impervious materials and surrounding soil). During dry conditions, the boundary conditions represent the situation represented in Figure 1, left. Since there is a radiation term that needs to be

modelled, the system of equations that we solve is transformed in a non-linear system that requires the use of the MINPACK FORTRAN library (Moré, et al., 1980) to solve it.

During wet conditions, the implicit scheme is coupled with an explicit scheme that predicts the mass and temperature of water on top of the surface at each time step. Heat transfer processes modeled during this stage are free convection between water and surface, and evaporative cooling and forced convection between water film and atmosphere (Figure 1, right). Since this is a weak coupling between surface and water, time step has to be adjusted accordingly because large temperature gradients lead to situations not possible physically (i.e. temperature of the water larger to the surface temperature). In order to create a more robust scheme in the future, it is planned that the model will include a spatial discretization of the water film and time integration of water mass and temperature schemes into the 1D surface temperature implicit model.

In order to compare SURF-TEMP results with the developed Python code and experimental/field measurements during wet conditions, we implemented several evaporative models (model 5 and model 6) into the water mass and temperature models.

3. Results

Based on the methods explained above, simulations are run in the Python code with various evaporation models, convective heat transfer coefficients, wind speeds, humidity, surface temperature and water heights. The goal is to understand the model's internal uncertainty (evaporation models and convective heat transfer coefficients) and sensitivity to different external factors (wind speeds, humidity, and surface temperature). Finally, the evaporative cooling effect with different initial water height is simulated with the aim to model the optimal watering rate.

3.1 Test on different evaporation models

Results obtained with the different evaporative cooling models are detailed in this section. The simulation is performed under the same condition (initial water height is 1 mm, v=1 *m/s*, convective heat coefficient model: Ashrae, 1993, RH=0.35). Our simulation shows that some models over predict the evaporative heat flux, while others produce much lower heat fluxes, as shown in Figure 4. The flux differences between different models can be about 2 times. For example, under the same condition, model 5 simulates 1250 W/m^2 evaporative heat flux but model 6 only shows 700 W/m^2 for the same flux. Yet, regardless of the model chosen, when the added water depth is 1mm, thirty minutes is not long enough to vaporize all the water under the given condition. Therefore, surface temperature keeps reducing due to continuous evaporative cooling. The magnitude of the evaporative flux is directly linked to the magnitude of reduction in surface temperature (Ts). That is, models that simulate high Qe values (model 1, 2, and 5) have stronger evaporative cooling effect than models that simulate lower Qe (mod 6 and 8). Thus, the simulated cooling efficiency depends on the chosen evaporation model.

Almost all models show that evaporative flux is stronger at the beginning of the simulation. For instance, the evaporative flux of model 5 starts around 1250 W/m^2 and reduces to 900 W/m^2 at the end. The reason is that the evaporation is higher due to the higher vapor pressure gradient at the beginning. The higher vapor pressure gradient is a result of the higher temperature difference between the water (T_w) and the air (T_0).

Despite the different values of evaporative heat flux simulated by the models, the changes of evaporative heat flux with time show similar behaviors. Therefore, to proceed with the analysis, evaporation model 1 is chosen as the benchmark for the tests in the sections below.

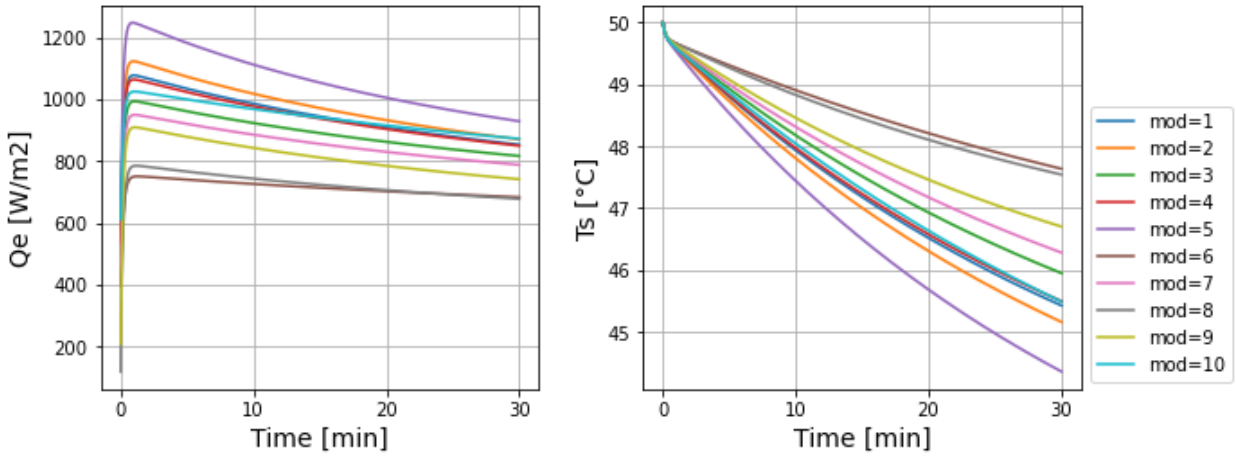

Figure 4. Simulated evaporative flux and surface temperature by the Python model (v=1m/s, convective heat coefficient model: Ashrae, 1993, RH=0.35, initial water height = 1mm)

3.2 Test on different convective heat transfer coefficient

This section analyzes the uncertainty of convective heat transfer coefficient (h), which is a key term in modelling evaporative cooling processes. According to Table 3, the evaporative heat flux is proportional to convective heat transfer coefficient in most models. Therefore, choosing the best equation that fits the corresponding condition will enhance model accuracy. The convective heat transfer coefficient is usually modelled as a linear function of wind speed. However, there is no concrete agreement in the constants used in the linear relation. The most common linear equation for the convective heat transfer coefficient with a low wind speed condition (v < 5 m/s) are listed in Table 2.

Figure 5 shows that the difference among the coefficient is around 1-1.5 times depending on the wind velocity. The relative difference is most distinct when the wind speed is close to zero, where there is a 50% difference between (Kusaka, et al., 2001) and (Palyvos, 2008) models. In addition, we obtained evaporative heat fluxes using different convective heat coefficients while maintaining weather conditions (v=1m/s, RH=0.35). The test is only performed with evaporation model 1 because similar behavior is expected with the other evaporation models. The different convective heat transfer coefficients directly lead to the divergence in evaporation rate estimation, as shown in Figure 6. Among the three models, (ASHRAE, 1993) yields values between the other two models, so it is the most neutral model and selected for the use in future simulation work.

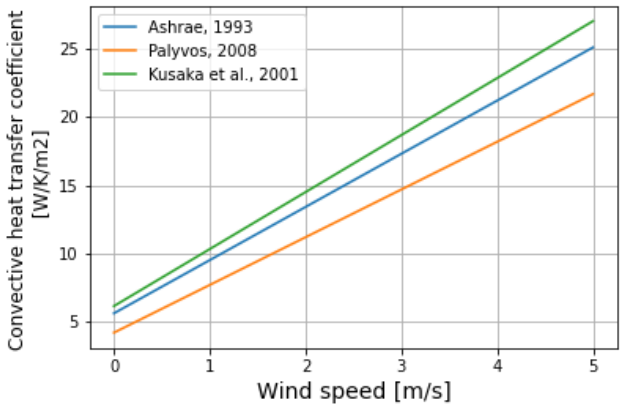

Figure 5. Convective heat transfer coefficients modelled by three different linear functions

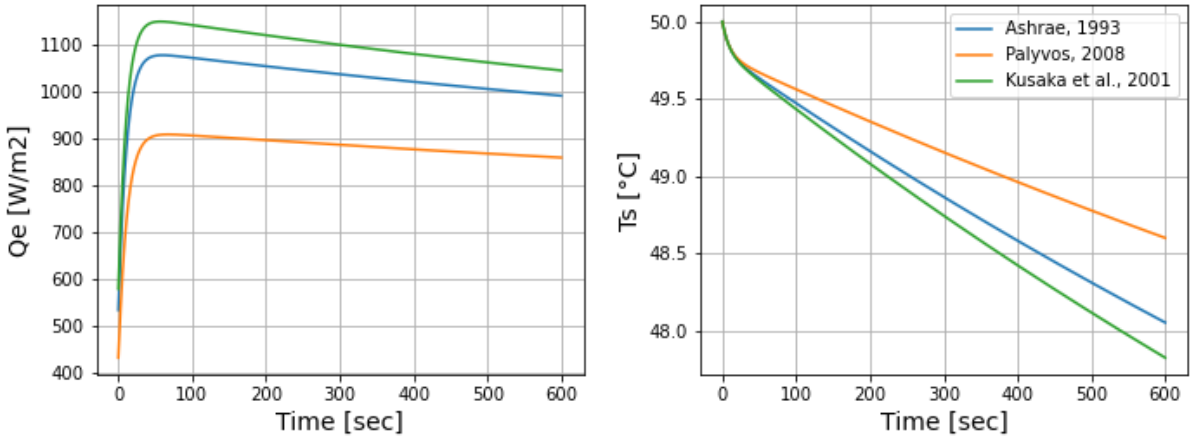

Figure 6. Evaporation rate using different convective heat transfer coefficients by the Python model (evaporation model=1, v=1m/s, RH=0.35, initial water height = 1mm)

3.3 Test on different wind speed

The results of model sensitivity to wind speed are presented in this section. As shown in Figure 5 in the previous section, wind speed has a strong influence on the convective heat transfer coefficient (h). Even within the small range of the common wind velocity in an urban environment (0 to 5 m/s), the resulted convective heat transfer coefficient (h) ranges from 3 up to 27 $W/m^2 \cdot K$. Therefore, wind speed has to be considered during the study. The simulation is run with the same water height (1 mm), evaporation model (model 1), relative humidity (0.35) and convective heat coefficient model (ASHRAE, 1993) with wind speed from 0 to 5 *m/s*.

As shown in Figure 7, wind speed is a crucial factor in deciding pavement cooling efficiency. When the wind speed is zero, the evaporative heat flux is only 700 W/m^2 and surface temperature reduction is less than 2 °C after 30 minutes. As we increase the wind speed up to 5 m/s, evaporative heat flux can reach 2250 W/m^2, and the maximum surface temperature reduction reaches more than 9 °C. Under the wind speed of 5 m/s, 1 mm of water evaporates in 25 minutes, so the surface temperature (Ts) starts to rise near the end of simulation, as shown in the right panel of Figure 7. Therefore, although a higher wind

speed reduces surface temperature more efficiently, the duration of the cooling effect still relates to water availability. Thus, it is important to consider both wind conditions and watering rate to achieve the desired evaporative cooling effect.

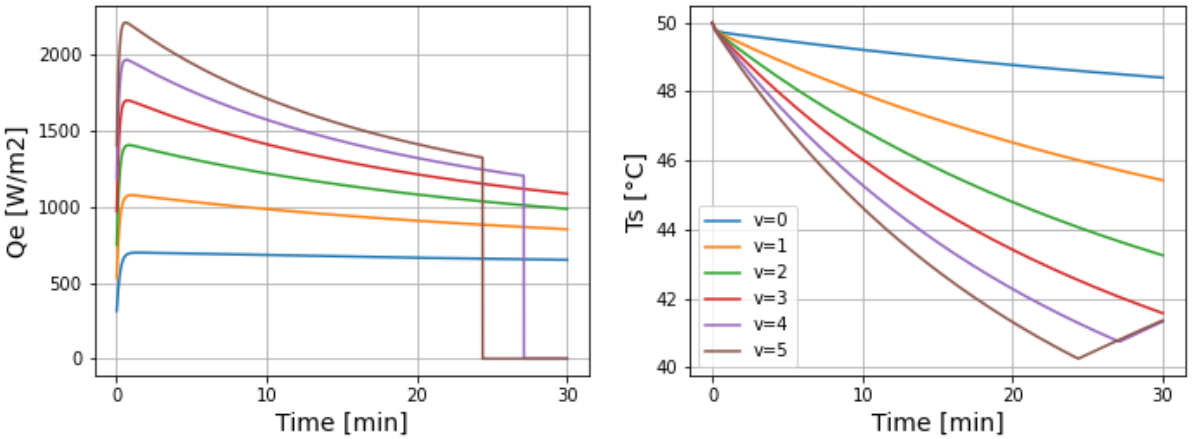

Figure 7. Influence of wind speed on evaporative heat flux and surface temperature by the Python model (evaporation model=1, RH=0.35, initial water height=1 mm, convective heat coefficient model: Ashrae 1993)

3.4 Test on different humidity

The results of sensitivity of evaporative cooling to relative humidity is presented in this section. As shown in Table 3, all evaporative models considered in the study consider the atmospheric relative humidity for evaporation mass rate calculations. These models agree that higher atmospheric relative humidity reduces evaporation. To perform the sensitivity test, the simulation is run with the same evaporation model (model 1), wind speed (v=1 *m/s*), convective heat coefficient model (ASHRAE, 1993), initial water height (1 mm), within a relative humidity from 0.3 to 0.9.

Figure 8 shows that although higher humidity does hinder evaporation, its influence is not as large as wind speed. Within a relative humidity from 0.3 to 0.9, a common range of relative humidity in European cities in summers, the evaporative heat flux and surface temperature differs by 400 W/m^2 and 3 °C at their maximum respectively. Besides, although low initial relative humidity of air causes higher evaporation, the atmospheric relative humidity increases during the evaporation process and reduces the evaporation rate (not simulated in our model). Thus, relative humidity is another main factor in deciding whether to conduct pavement watering and thermal comfort in cities.

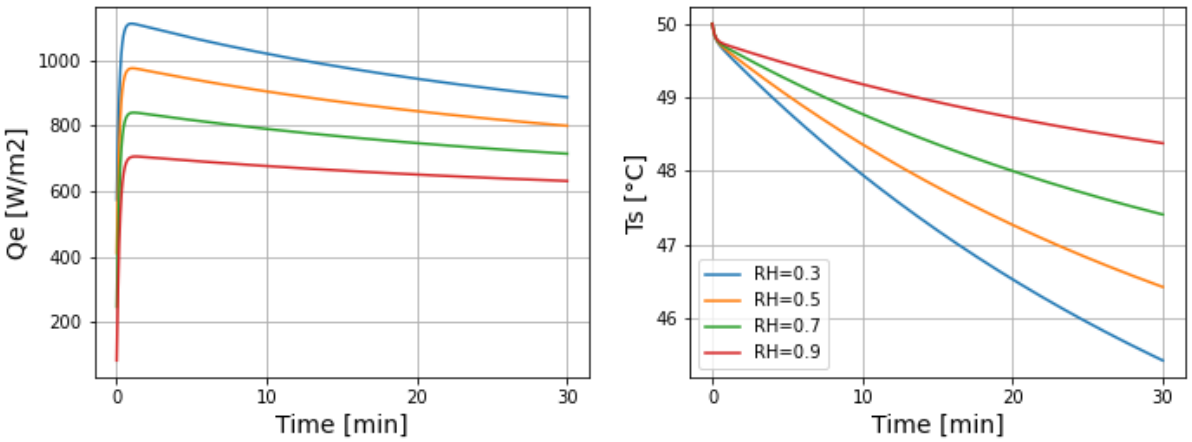

Figure 8. Influence of relative humidity on evaporative heat flux and surface temperature *by the Python model (evaporation model=1, v=1m/s, convective heat coefficient model: Ashrae 1993, initial water height =1 mm)*

3.5 Test on different surface temperature

In this section, we aim to assess the cooling effect on three surfaces with initial surface temperature of 50, 45, and 40 °C respectively under the same air temperature (35°C). According to Eq (17), the saturation vapor pressure increases exponentially with temperature. Because air near the water surface is assumed to be saturated (RH=1) and has the same temperature as the water, its saturation vapor pressure increases with the water temperature. Therefore, a higher evaporation rate is expected when the pavement surface temperature is higher given the same weather condition.

The simulation is run with the same evaporation model (model 1), convective heat coefficient model (ASHRAE, 1993) ,wind speed (1 m/s), relative humidity of air (0.35), initial water height (1 mm). Results are shown in Figure 9. The difference of evaporative heat flux under different initial surface temperature is significant. Initial surface temperature of 50°C gives a maximum evaporative heat flux about 1080 W/m^2 while Initial surface temperature of 40°C gives about 650 W/m^2. Thus, the cooling effect is strongest when the initial surface temperature is higher. Surface cooling reaches 4 °C when the initials surface temperature (Ts) is 50 °C. When the initial surface temperature is only 45°C, the cooling effect only reduces the temperature by 1.5 °C. When the surface temperature is 40°C, the evaporative cooling is not even strong enough to prevent the surface temperature from rising due to the large incoming radiative heat flux.

Thus, the simulation proves that evaporative cooling is stronger when the surface temperature is higher. As a result, if a large reduction of surface temperature is the goal, pavement cooling should be conducted on the area where surface temperature is high enough.

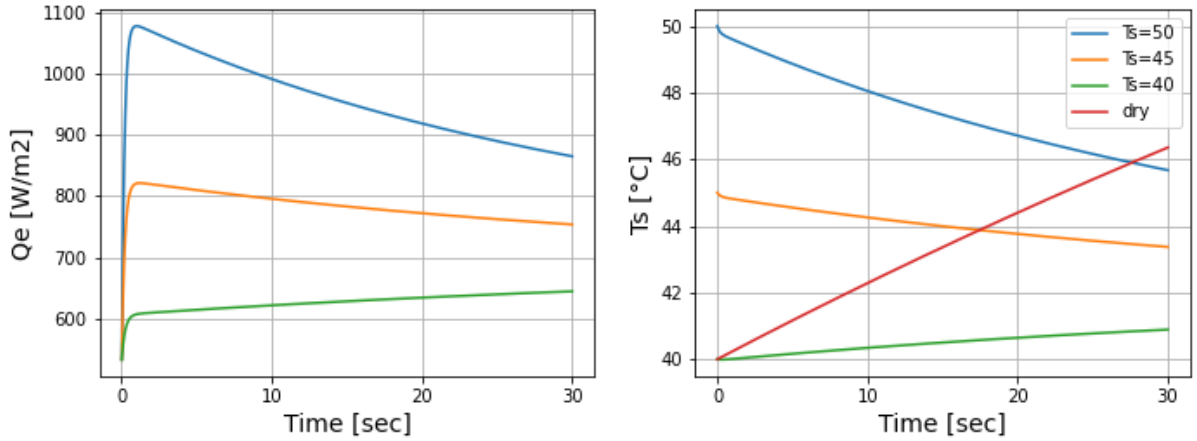

Figure 9. Influence of initial surface temperature on evaporative heat flux and surface temperature *by the Python model in comparison with dry condition. (evaporation model=1, v=1 m/s, RH=0.5, convective heat coefficient model: Ashrae 1993, initial water height =1 mm)*

3.6 Test on initial water height and optimal watering rate

After performing the uncertainty and sensitivity test, we continue to simulate the cooling effect of several initial water heights on the surface temperature with the goal of identifying the optimal watering rate. With the water only added once at the beginning of the simulation, we tested the evaporative cooling effect during one hour with the same wind speed (1 m/s), relative humidity (0.35), convective heat coefficient model (ASHRAE, 1993), with initial water heights from 0.25 mm to 2 mm.

Focusing on the lowest water amount that is tested (0.25mm), Figure 10 shows the resulted evaporative heat flux (Qe) and surface temperature (Ts) from the 10 evaporative models. When the sprayed water is only 0.25 mm, the water vaporizes within 10 minutes in the models that estimate higher evaporative heat flux (model 1,2,4, and 5) with the weather condition above. In case where there is no more water on the pavement, the evaporative heat flux (Qe) becomes zero and there is no evaporative cooling effect and surface temperature starts to rise. The cooling effect at the end of simulation is about 1.7 °C estimated by model 5 and the minimum is around 0.9°C simulated by model 6.

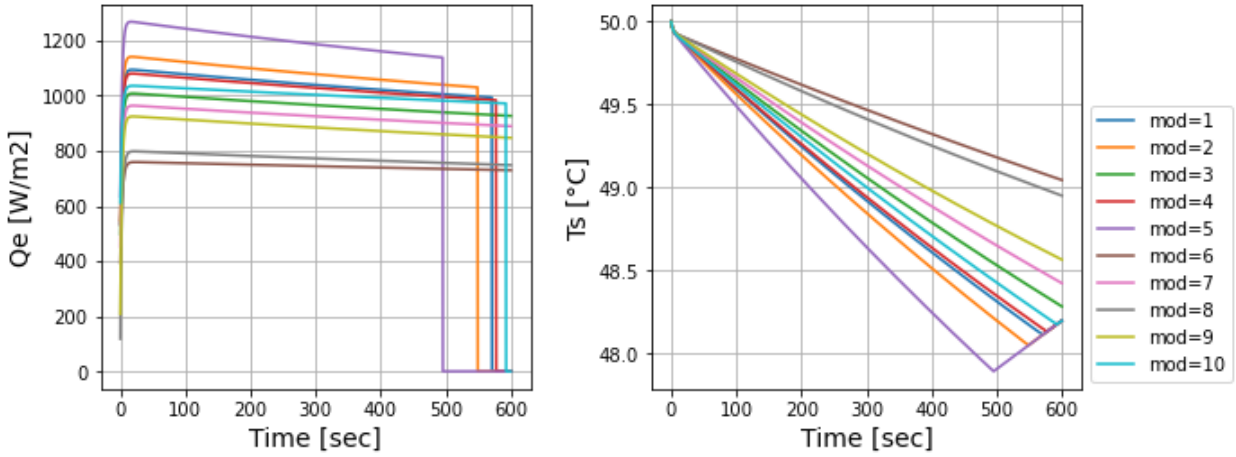

Figure 10. Simulated evaporative flux and surface temperature when the initial water height is 0.25 mm by the Python model (v=1m/s, RH=0.35, convective heat coefficient model: Ashrae, 1993)

Proceeding to test a higher initial water height of 1 mm, the simulation results from the ten evaporative models are shown in Figure 11. It shows that even with the model that simulates the highest evaporative heat flux, water still presents until the end of simulation. Therefore, the evaporation is continuous throughout the simulation and cooling effect keeps reducing the pavement surface temperature.

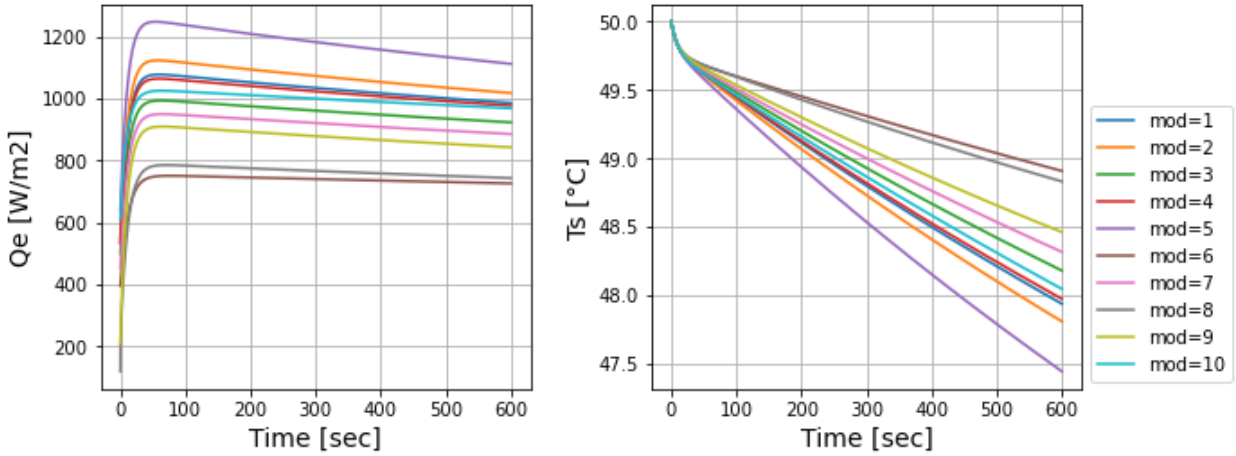

Figure 11. Simulated evaporative flux and surface temperature when the initial water height is 1 mm by the Python model (v=1m/s, RH=0.35, convective heat coefficient model: Ashrae, 1993)

Comparing the results in Figure 10 and Figure 11, 0.25 mm of water only reduces Ts by 0.9 to 1.7 °C (depending on the evaporation models), while 1 mm of water reduces Ts by 1.1°C to 2.5°C. Therefore, a higher initial water height enhances the evaporative cooling. When the initial water height is only 0.25 mm, due to the smaller amount of water, the pavement surface dries out and its temperature starts to rise. Thus, a sufficient water height to keep the pavement wet is necessary if a higher temperature reduction is desired. Yet, increasing watering rate cannot increase cooling effect infinitely and the higher watering rate also create larger burden on water resource ((Hendel, et al., 2015) & (Parison, et al., 2020)). Therefore, the watering rate that is just enough to keep the pavement surface wet during the whole simulation is called the optimal watering rate.

As shown in Figure 10 and Figure 11, model 5 and model 6 simulated the largest and smallest evaporative heat flux respectively. Therefore, these two models are chosen for the tests to quantify the range of uncertainty regarding the optimal watering rate in the following section. Simulation is performed with the weather condition described before. Simulated results of the two models are shown in Figure 12 and Figure 13 respectively.

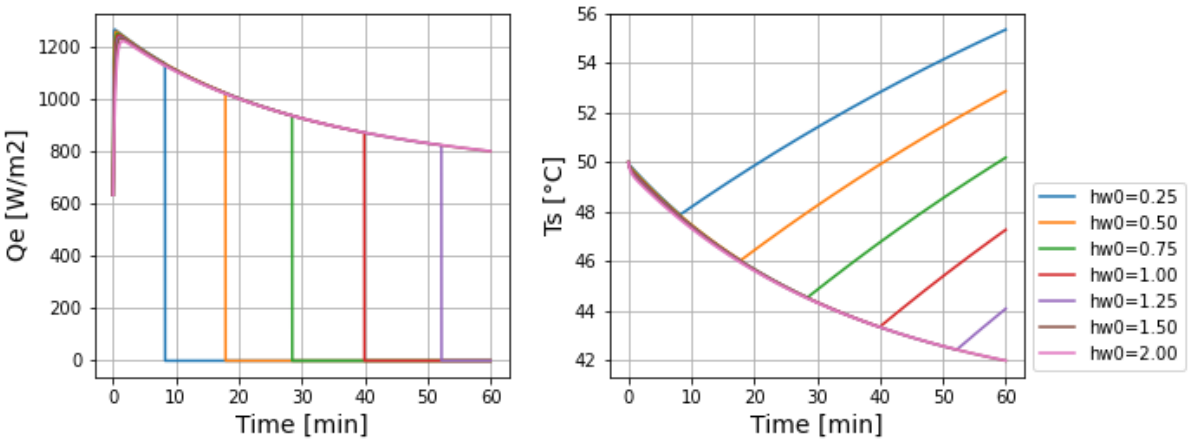

Figure 12. Evaporative heat flux and surface temperature during one hour of simulation by the Python model (Evaporation model = 5, v=1m/s, relative humidity =0.35, convective heat coefficient model: Ashrae 1993)

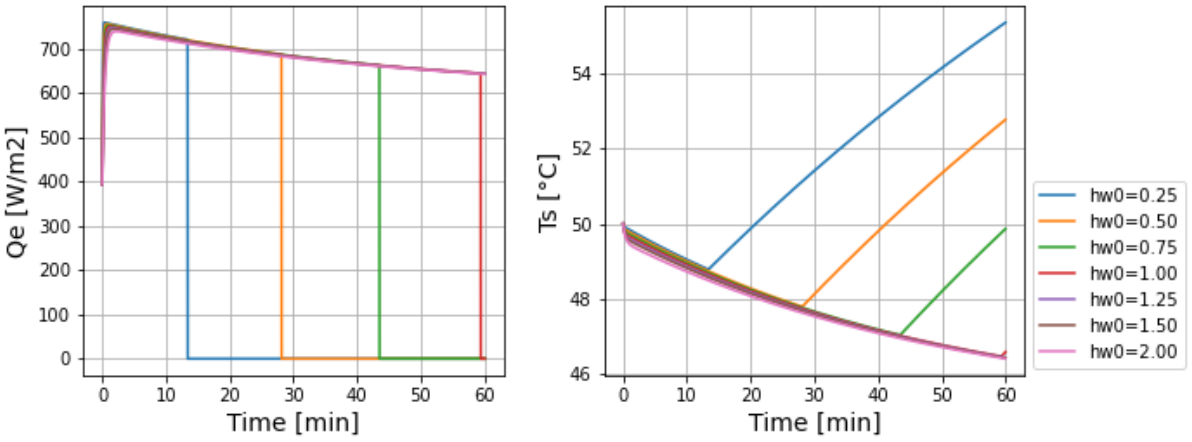

Figure 13. Evaporative heat flux and surface temperature during one hour of simulation by the Python model (Evaporation model = 6, v=1m/s, relative humidity =0.35, convective heat coefficient model: Ashrae 1993)

Figure 12 shows that when the added water is lower than 1.25 mm, model 5 simulates that the water totally evaporates within one hour. Once there is no water on the pavement, its surface temperature (Ts) starts to rise. On the other hand, when the watering rate is above or equal to 1.5 mm/hr, the results of their evaporative heat flux and temperature reduction are the same. Thus, increasing added water height above 1.5 mm does not increase cooling effect. Therefore, the water that can create the largest surface temperature reduction without wasting water resource, or so-called optimal watering rate estimated by evaporation model 5 is between 1.25 and 1.5 mm/hr under this weather condition.

Figure 13 shows the same graph for the results of model 6. Comparing Figure 12 and Figure 13, model 6 simulates lower evaporative heat flux and smaller surface temperature reduction at all watering rates. This is expected as the results shown in Figure 4 before. Due to the lower evaporative heat flux simulated by model 6, the water stays upon the pavement longer time until it fully evaporates. Thus, Figure 13 shows that there is still water at the end of simulation if the watering rate is above 1 mm/hr. For watering rate higher than 1 mm/hr, the same cooling effects are resulted. Therefore, the optimal watering rate is found

near 1 mm/hr. Comparing to 1.25 to 1.5 mm/hr of model 5, this is a much smaller value. Also, the lower evaporative heat flux simulated by model 6 also results in lower cooling effect than model 5 (maximum surface temperature reduction of 8 °C and 3.6 °C respectively.)

4. Model Validation

In this chapter, we validated the simulations results of our Python code and the SURF-TEMP with several existent theoretical models, lab measurement, and field observation on surface evaporative heat flux and surface temperature during evaporative cooling. We start with validating the Python code, and proceed to the SURF-TEMP.

4.1 Validation of the Python code with a theoretical model

To evaluate the correctness of the models, the resulted water temperature and heat fluxes are compared with the theoretical simulation in (Min & Tang, 2015). (Min & Tang, 2015) established a theoretical model to simulate thin water film evaporation on an adiabatic surface. They theoretically model and analyze evaporative heat flux and temperature of water film when there is no radiation input, and the air has constant temperature and humidity.

Because (Min & Tang, 2015) consider a water film with no radiation input (R) nor pavement conduction (Q_{cond}), we turned the two fluxes to zero in the Python model for more accurate comparison. The convective heat transfer coefficient (h) in our simulation also increases to a fixed value of 100 $W/m^2 \cdot K$ as the value in the literature. The main remained difference in the setting is that convection ($Q_{conv,sw}$) exists between water and pavement in our simulation, while the interface is considered adiabatic in their work. Because the convective flux ($Q_{conv,sw}$) is an important flux to examine, we did not change it according to their setting. Also, the water film in their simulation is discretized and has different temperatures at different depth, but water temperature is assumed to be constant with height in our model. As in Chapter 3, evaporation model 1 is chosen for illustration. The simulation is run for three initial water heights 0.1 mm, 0.5 mm, and 1.0 mm as in (Min & Tang, 2015). The resulted water temperature (Tw) and evaporative heat flux (Qe) in comparison with the results in (Min & Tang, 2015) are shown in Figure 14 and Figure 15 respectively.

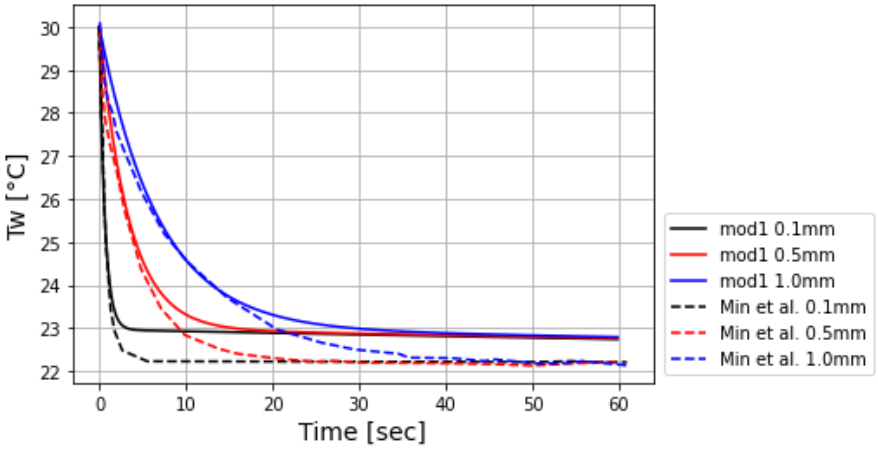

Figure 14. The simulated water temperature (Tw) by the Python model in comparison with (Min & Tang, 2015) *(evaporation model=1, relative humidity=0.35, convective heat transfer coefficient=100 W/k·m2)*

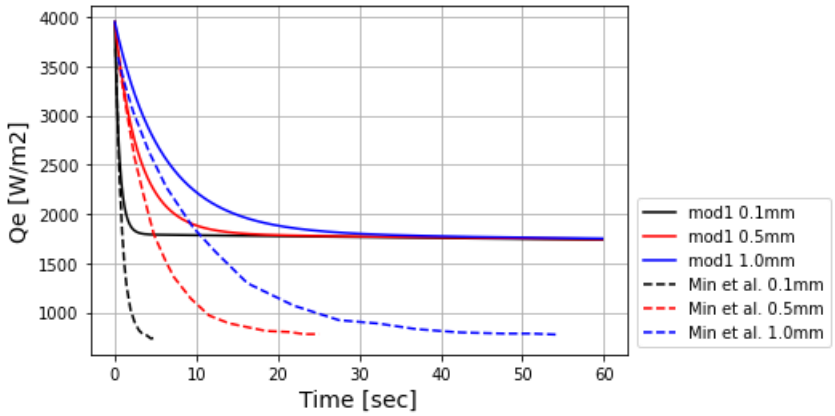

Figure 15. The simulated evaporative heat flux (Qe) by the Python model in comparison with (Min & Tang, 2015) (evaporation model=1, relative humidity=0.35, convective heat transfer coefficient=100 W/k·m2)

As shown in Figure 14, the changes of water temperature over time in our simulation and their model show high similarity. Water temperature reduces within one minute to reach equilibrium. Water temperature drops quicker when the water is thinner, which is also identical to the results in (Min & Tang, 2015). Yet, the equilibrium temperature of our simulations and (Min & Tang, 2015) are not identical due to the different boundary conditions. They assume the interface between water and surface is adiabatic while there is a convective heat flux in our model.

Because the main cooling flux in the system is the evaporative heat flux, the change in temperature is mainly caused by evaporative heat flux (Qe). Therefore, evaporative heat flux (Qe) and water temperature (Tw) shows similar variation with time, as shown in Figure 15. Again, it displays the same behavior as (Min & Tang, 2015), that the thinner the initial water height, the shorter time required for evaporative heat flux to reach equilibrium. The difference in equilibrium evaporative heat flux is again the consequence of the different boundary condition. Noted that in their work, simulation time is shorter for thinner water, so their three simulation ends at different times.

Because of the distinct difference between the evaporative flux at the beginning of the simulation and after, the authors divide the evaporation process into two stages. The unsteady stage where the evaporative rate decreases and the steady stage where the evaporative rate is constant. The description on the two stages is described in Table 4.

Table 4. Comparison between the unsteady and steady stage during evaporative cooling (Min & Tang, 2015)

Stages	Unsteady stage	Steady stage
Occurrence time	within the first 30 seconds after water is sprayed on the surface, depending on water thickness (0.1 to 1.0 mm)	after the unsteady stage
Evaporation rate	keeps decreasing	stabilizes
Water temperature	keeps reducing	stabilizes

With the high similarities between our Python model and (Min & Tang, 2015), the thermodynamic and structure of our Python model is verified.

4.2 Validation of the Python code with lab and field data

After validating our simulations with the theoretical model, we further compared them with measured data in lab and field. Several field and one lab measurements on evaporative heat flux from watered surface in existent literature are referred for comparison and validation.

First, (Qin & Hiller, 2016) performs a field watering experiment to measure evaporation from pervious concrete and surface temperature variation. Similar to the findings in the theoretical model (Min & Tang, 2015), higher evaporation rates shortly after initiating the watering of surfaces are also found in their field campaign, as shown in Figure 1 in the Supplementary Figures. Their measured evaporation rate is highest shortly after water is added and decreases exponentially as water drains out. The curve of the evaporation rate is similar to our simulation (e.g., Figure 4). In their results it is shown that evaporation lasts longer since pervious materials can hold water for a longer time than the impervious surface modelled in our simulations.

Second, a similar approach was performed by (Nayak, et al., 2020). They measured evaporative heat flux above impervious asphalt surface after precipitation with the goal to develop a numerical model. Their measurement also shows an exponential decreasing curve of evaporation rate from 200 to 50 $W/m^2$with the maximum happens right after precipitation. Their results are shown in Figure 2 in the Supplementary Figures.

The effect of different water amount on the pavement cooling is also validated with the lab data from (Parison, et al., 2020). They measured evaporative heat flux from asphalt pavement surface in a climate chamber with controlled watering rate, radiation, and air temperature. They aimed to obtain the optimal watering rate for pavement evaporative cooling by testing watering rates from 0.1 to 3.0 mm/hr.

In their experiment, fixed amount of water equal to 0.05 mm height is sprayed with a sprinkler each time. Total watering height per hour is adjusted by changing the watering frequency. From their research, a higher watering rate increases the evaporative cooling flux, but only until a certain watering rate. Beyond the certain watering rate (optimal watering rate), extra water can no longer enhance evaporate heat flux, so its effect on pavement cooling is marginal. They measured average evaporative heat flux by calculating energy balance of pavement surface with the measurement of other fluxes involved (radiative heat flux, conductive heat flux, and convective heat flux between pavement and air) in the system. We ran the Python model with very similar inputs as their experimental conditions (relative humidity is 0.35, air temperature is 35°C, and convective heat transfer coefficient is 9.5 and 10 in our model and their experiment respectively). Our simulated average evaporative heat fluxes with model 5 and 6 (i.e., Figure 10 and Figure 11 in section 3.6) are compared with their lab measurement under different watering rates from 0.25 to 2 mm per hour. The main setting difference is that in their experiment water is sprayed periodically whereas the same total volume of water is only added at the beginning of our simulation (because the Python model does not have the input option to adjust water frequency, which is later improved in the SURF-TEMP model). To compare with their observed average evaporative heat flux, we calculated the average evaporative heat flux within one hour including zero values (when the surface is dry). The reason of including the zero values is that it is the same method to measure average evaporative heat flux in (Parison, et al., 2020). The comparison among our simulation results and the literature results are shown in Figure 16.

Figure 16 shows that for watering rates lower than 0.75 mm/hr, the modeled evaporative heat fluxes are similar to values measured in lab condition. This is because all the sprayed water evaporates in a short time at such low watering rates (both in the simulation and in the lab). So there are many zero values in

the simulated and lab-measured evaporative heat fluxes which let their averages become close. This also explains why model 5 and model 6 simulates similar values of evaporative heat flux when watering rate is lower than 0.75 mm/hr. For watering rate above mm/hr, the water is enough to keep the pavement surface wet during the whole simulation period (1 hour), so the simulated evaporative heat fluxes are different from each model (as also shown in Figure 4 in section 3.1), and their difference with (Parison, et al., 2020) enlarges. Even model 6, the model that simulates the lowest evaporative heat flux among the ten evaporation models overestimates the flux.

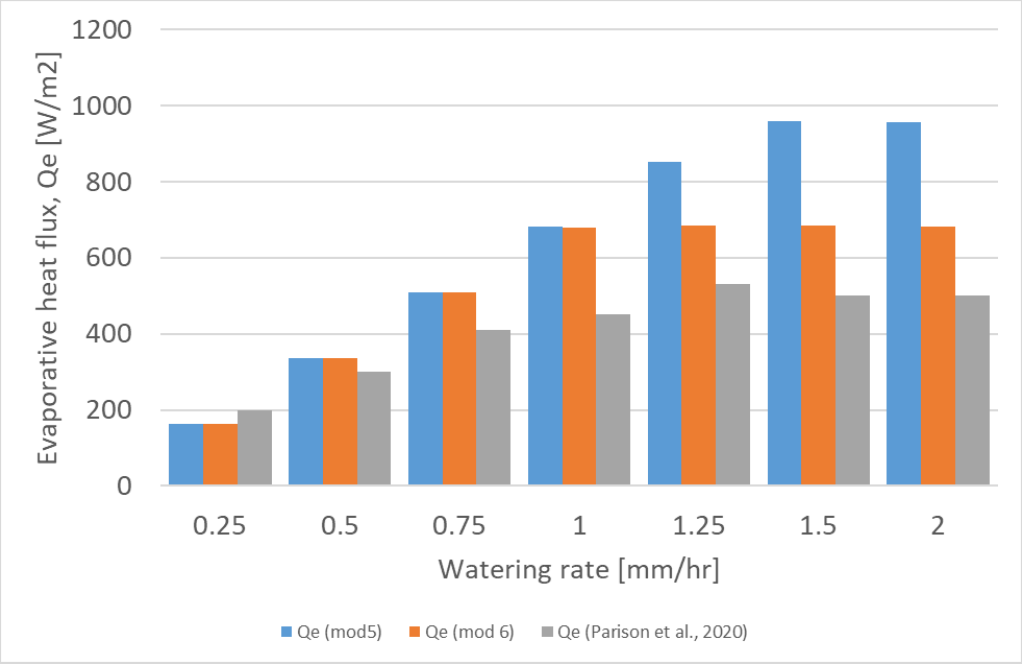

Figure 16. Comparison of evaporative flux against water rate among our simulation by model 5 and 6 by the Python model and lab measurement from Parison et al., 2020

In summary, the simulated results with the initial water height of 1 mm are compared with 1 lab measurement and 3 field measurement and summarized in Table 5. The results show that our Python models overestimate the evaporative cooling flux, especially comparing to field measurement.

Table 5. Summary of the comparison among our simulation results by the Python model, lab measurement, and field measurement

Quantity of interest	Unit	Our models	Lab measurement (Parison, et al., 2020)	Field measurement (Hendel, et al., 2015)	Field measurement (Nayak, et al., 2020)	Field measurement (Qin & Hiller, 2016)
Reduction in surface temperature (ΔTs)	°C	~3	5	13	4.5 ~ 5.5	10
Initial surface temperature (Ts)	°C	50	50	50	30	60
Evaporative flux, Qe	W/m2	680	470	224	130~150	500
Net surface radiation, R	W/m2	~750	~750	~800	~600	~800
Sprayed water temperature	°C	35	35	20-25	N.A	N.A
Sprayed water height	mm	1	1	1	0.167 mm/minute for 30 minutes	N.A
Surface material	Asphalt					Pervious concrete pavement

4.3 Validation of SURF-TEMP with lab and field measurement

After performing the uncertainty and sensitivity tests and validation of the Python model, we proceed to validate the SURF-TEMP model. As shown in Figure 4, model 5 and model 6 simulates the largest and smallest evaporative heat flux respectively. Therefore, these two models are chosen for validating SURF-TEMP to quantify the range of uncertainty. Simulation performed by SURF-TEMP are run for longer time periods than the Python code and compared with results the literature.

One advantage of the SURF-TEMP model is that watering frequency can be adjusted. Thus, the watering rate and frequency are adjusted according to the same values in (Parison, et al., 2020) for the best possible comparison. (Parison, et al., 2020) uses a sprinkler that sprays 0.05 mm of water at each spray to adjust hourly watering rate. For instance, when the hourly watering rate is 1 mm, the sprinkler sprays per 3 minutes; when the hourly watering rate is 2 mm, the sprinkler sprays per 1.5 minutes. The convective heat transfer coefficient, and relative humidity are set 10 $W/m^2 \cdot K$, and 0.35 respectively since these are the same values as in the literature. The shortwave radiation and longwave radiation are set as 1200 W/m^2 and 180 W/m^2 during the first eight hours (so called day phase). They become 0 W/m^2 and 450 W/m^2 after the first eight hours (so called night phase). The simulation is first run for ten hours with no

watering to model surface temperature during dry condition. Then, the simulation is run for eight hours with seven different watering rates varies between 0.25 and 2 mm/hr to analyze optimal watering rate.

Two representative simulated results performed by model 5 with watering rate 0.75 mm/hr and 1.5 mm/hr are shown in Figure 17 and Figure 18 for illustration. Figure 17 shows that watering rate of 0.75 mm/hr eventually reduces the surface temperature by 5.5 °C at the end of day phase. The spikes in the wet case are caused by the frequent watering and drying out of the surface. It also indicates that the pavement surface is not continuously wet with this watering rate. Comparing to the results in (Parison, et al., 2020), the spikes are also visible, as shown in Figure 3 in the Supplementary Figures section. Despite of this similar behavior between our modeled results and their lab observation, the temperature reduction compared to the dry case at 8 hours is much lower in our simulation than the in the lab measurement (5.5 °C versus 15.8 °C).

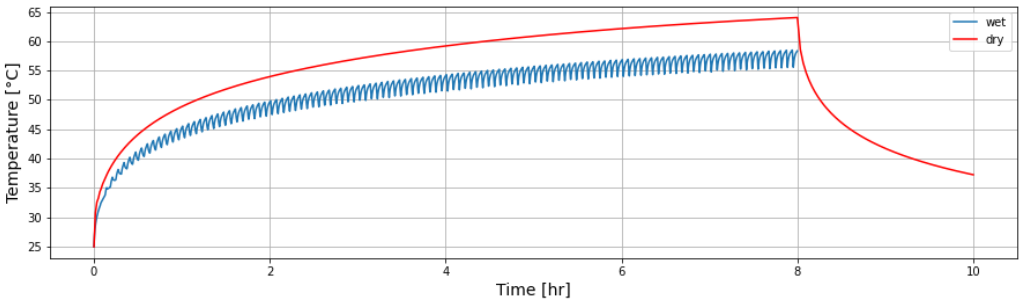

Figure 17. Simulated pavement surface temperature by SURF-TEMP with watering rate 0.75 mm/hr and period of 4 minutes (evaporation model=5, RH=0.35, convective heat transfer coefficient = 10 W/m2·K)

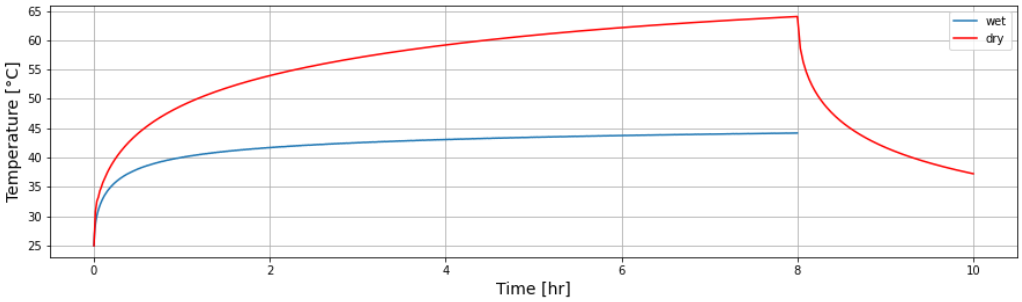

Figure 18. Simulated pavement surface temperature by SUR-TEMP with watering rate 1.5 mm/hr and period of 2 minutes (evaporation model=5, RH=0.35, convective heat transfer coefficient = 10 W/m2·K)

When the watering rate increases to 1.5 mm/hr, the temperature reduces significantly about 19.7 °C at 8 hours compared with the dry case. Comparing the simulation results of two watering rates in Figure 17 and Figure 18, final temperature reduction increases 3.6 times by doubling the watering rate from 0.75 to 1.5 mm/hr. Besides, the temperature spikes do not occur with this higher watering rate because the surface is constantly wet. Still, even with the higher temperature reduction, it is slightly smaller than the measured reduction (22.3 °C) in (Parison, et al., 2020).

Results of all simulations are detailed in Table 6. For each watering rate, two evaporative heat fluxes are calculated. Qe is the average evaporative heat flux, including zero values when the surface is dry. $Q_{e,wet}$ calculates the average value only when the pavement is wet excluding zero values. The results are also plotted in Figure 19 in comparison with (Parison, et al., 2020).

Table 6. Simulation results of evaporative heat flux and surface temperature reduction from evaporation model 5 and 6 by SURF-TEMP. (Convective heat transfer coefficient is 10 W/m2K, RH=0.35)

	Watering rate $[mm/hr]$	0.25	0.5	0.75	1	1.25	1.5	2
	Frequency [min]	12	6	4	3	2.4	2	1.5
model 5	$Q_{e,wet}$ $[W/m^2]$	903	869	812	533	532	531	531
	Qe $[W/m^2]$	65	130	198	533	532	530	530
	ΔTs [°C]	1.5	3.5	5.5	19.7	19.8	19.8	19.8
model 6	$Q_{e,wet}$ $[W/m^2]$	458	441	367	365	363	362	363
	Qe $[W/m^2]$	65	130	366	365	364	362	362
	ΔTs [°C]	1.5	3.4	13	13.4	13.5	13.6	13.6
Parison et al, 2020	Qe $[W/m^2]$	200	300	410	450	530	500	500
	ΔTs [°C]	6.5	12.6	15.8	15.9	18.1	22.3	21.1

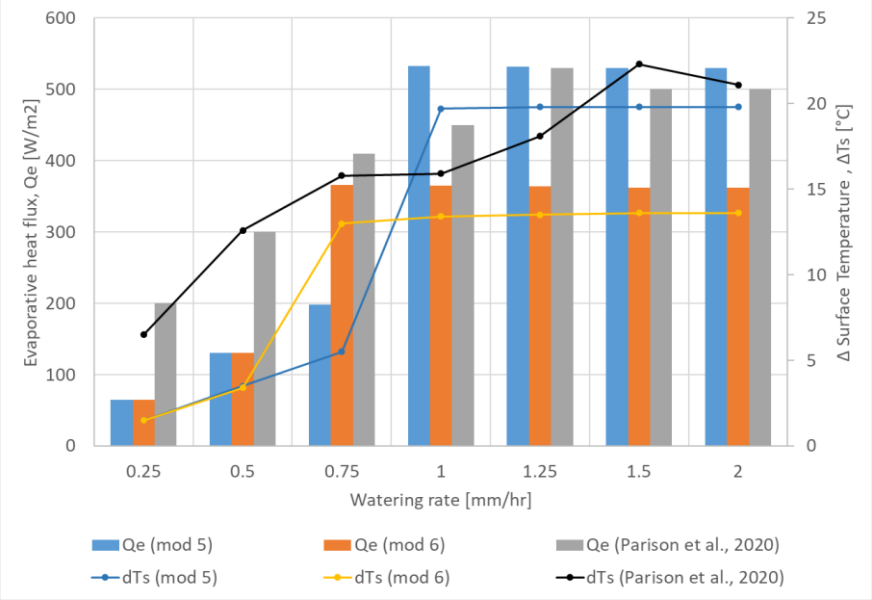

Figure 19. Evaporative heat flux and surface temperature reduction under different watering. Comparison of the SURF-TEMP simulated results using evaporation model 5 and 6, and lab measurement from (Parison et al., 2020)

Figure 19 shows that model 5 simulates very similar evaporative heat fluxes and surface temperature reduction to lab measurement in (Parison, et al., 2020), when watering rate is equal or above 1 mm/hr. On the other hand, model 6 underestimates the fluxes and temperature reduction. However, when the watering rate is at 0.75 mm/hr, model 6 shows better agreement to the lab measurement than model 5. For watering rates equal or lower than 0.5 mm/hr, both models 5 and 6 fail to show alignment with the lab measurement.

5. Discussion

In this chapter, we discuss the main challenges in the research. Namely, first, the heat transfer model between pavement surface and water film; second, disagreement of simulation in our models and lab observation from existent literature.

5.1 Heat transfer model between pavement surface and water film

As described before in section 2.3, most existent pavement evaporative cooling models neglect the heat flux between the pavement surface and the water by assuming that they reach thermal equilibrium. Yet, in our simulation in section 3.1 to 3.4, initial temperature of the sprayed water is 35 °C and the pavement surface is at 50°C. Thus, we expect a strong heat flux between them, at least during the first few seconds/minutes after the water is sprayed on the pavement.

Figure 15 shows that the temperature between pavement surface and the water film approaches each other immediately once water is added on top of the surface. Particularly, the water temperature rises immediately about 10°C upon sprayed on the pavement. The rapid temperature change in the beginning of watering is observed in the field campaign of (Na, et al., 2021). They concluded that considerable evaporation and surface temperature reduction occur within the first ten minutes after watering under their experimental condition. This can be explained by our model that at the beginning of watering the heat convection between the water and the pavement is larger when their temperature differences are higher.

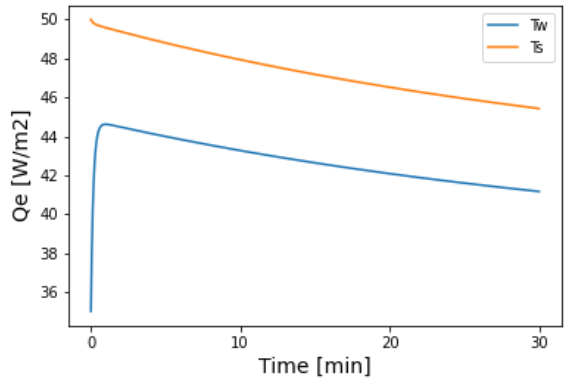

Figure 20. Simulated temperature of water film and pavement surface by the Python code when the initial water height is 1 mm (evaporation model=1, RH=0.35, v=1 m/s, convective heat coefficient model: Ashrae, 1993.)

On the other hand, Figure 20 shows that although both water and surface temperatures reduce as evaporation occurs, they do not reach thermal equilibrium within thirty minutes in our Python model. This is different from the field measurement of (Azam, et al., 2018). Under similar conditions as in the numerical simulation, they observed that the temperature between pavement surface and water reached equilibrium within 20 minutes after water was sprayed.

After analyzing water temperature variation in the Python model, we proceeded to analyze it in the SURF-TEMP model. With the same simulation condition as described in section 4.3, the simulated result from model 5 is shown in Figure 21 for illustration. Noted that water temperature is shown as zero when the pavement is dry. The peak of water temperature at the beginning is due to initialization of water temperature (35°C). Throughout the simulation period, it shows that if pavement surface temperature is higher than the temperature of sprayed water (35°C), pavement surface temperature reduces immediately after the water is sprayed on the pavement. Yet, like the Python model, a difference of around 4 °C exists between the two. Thus, the results also deviate with (Azam, et al., 2018).

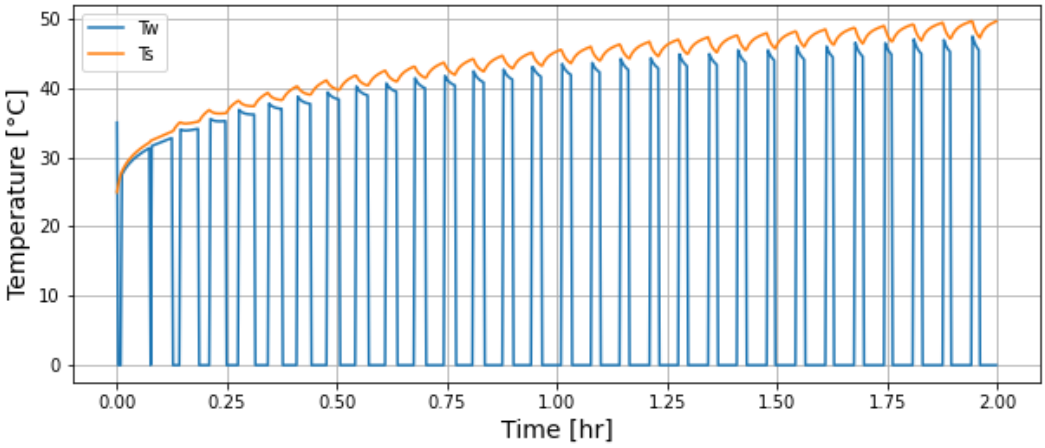

Figure 21. Simulated temperature of water film and pavement surface by SURF-TEMP (evaporation model 5, watering rate is 0.75 mm/hr, RH=0.35, convective heat transfer coefficient is 10 W/m2·K)

The final challenge with water temperature simulation is its validation. We only found one literature (Min & Tang, 2015) that models water temperature during evaporative cooling on pavement-like surface. Yet, their simulation on water temperature is not verified with actual lab or field observation either. Except (Azam, et al., 2018), most existent literature on lab or field measurement of evaporative cooling did not separately measure water temperature and pavement surface temperature during the evaporation. Therefore, it is difficult to validate our simulated results of water temperature and accuracy of the heat transfer model between water and pavement.

5.2 Disagreement in simulation and lab observation

As presented in chapter 4, there is a difference between actual measurement and the results obtained by our models. The possible reasons are discussed in this section.

First, the evaporation models in both models assume that the water does not infiltrate into the pavement and water film has an equal height above the pavement. Due to the unevenness of an asphalt surface, this assumption is not possible in practice especially when water height is low. For similar reason regarding pavement structure, unlike the evaporation models tested in this study, some other literature suggest that water content at the surface and pavement porosity should be considered on evaporative rate calculations ((Wei & He, 2013), (Nayak, et al., 2020) and (Qin & Hiller, 2016)). Therefore, the assumption that water is at equal height and no infiltration into the pavement may be the cause for our simulation discrepancy during low watering rates.

Second, when the water on top of the surface is thin, models for water evaporation from free surface (such as pools and ponds) are not applicable because they tend to overestimate evaporation rate (Tang & Etzion, 2004). Experimental results from (Tang & Etzion, 2004) suggest that evaporative rate is not a linear function of the vapor pressure gradient, but the function should be exponential with a power of 0.82. The uncertainty of the non-linear relation between evaporation and vapor pressure gradient, might be the cause to the inconsistency between simulation and observation.

Third, although the thermal properties of the pavement in the simulation are set equal to the material considered in the lab measurement, the simulated temperature does not show the exact variation as the measurement even under dry condition. As Figure 17 shows, surface temperature rises to 64°C in our simulation while it only rises to 61 °C in the lab measurement during the eight-hour day phase (Figure 3

in the Supplementary Figures). This is caused by the difference in initial temperature. (Parison, et al., 2020) placed the pavement column under night phase (air temperature 25 °C) for one day before the experiments to stabilize it, but we did not perform the same procedures in our simulation. Therefore, this may be another cause to the discrepancy between simulations and lab measurement.

6. Conclusion

We developed a Python model to simulate pavement evaporative cooling with adjustable weather variables and ten evaporation models available in the literature are included. We performed an uncertainty analysis of the selected evaporative cooling models and convective heat transfer coefficients, and sensitivity analysis on wind speeds, air humidity, surface temperature, and initial water height. Simulation results obtained by the Python code are validated with measurement found in existent literature. After these tests and validations are performed, two of the evaporative models that represent the upper and lower limits of the evaporative heat fluxes are added into the SURF-TEMP model. The SURF-TEMP model is compared with lab measurement by (Parison, et al., 2020) in order to validate the evaporative heat flux, surface temperature reduction, and optimal watering rate.

The main findings in the research are:

- Uncertainty analysis of the Python evaporative cooling model: Depending on the evaporation models used, the simulated maximum evaporative heat flux and surface temperature reduction can differ around two folds under the simulation condition,
- The equation in (ASHRAE, 1993) gives the most neutral estimation for connective heat transfer coefficient under urban heat wave condition,
- Sensitivity analysis of the Python evaporative cooling model: Wind speed, surface temperature, and atmospheric relative humidity are of high importance to optimize cooling effect and water resource,
- If watering rate is equal or higher than 1 mm/hr, lab measured evaporative heat flux and surface temperature reduction in (Parison, et al., 2020) are within the range given by the upper and lower limits simulated by SURF-TEMP. Yet, if watering rate is lower than 1 mm/hr, SURF-TEMP underestimates the evaporative heat flux and surface temperature reduction,
- Optimal watering rate: simulation results obtained by SURF-TEMP shows that the optimal watering rate is between 0.5 and 0.75 mm/hr for evaporation model 6, and between 0.75 and 1.0 mm/hr for evaporation model 5 under the same experimental condition as (Parison, et al., 2020).

With the findings above, improving the capability of SURF-TEMP at low watering rate would be the focus of future work. Recommendation is to improve the completeness of thermodynamic processes in the water-pavement interface. This can be achieved by:

- Discretize the water film: model the water temperature variation with height and include conductive heat flux between water and the pavement into the energy balance of the system,
- Model water movement: include a model for simulating pavement porosity, water content, and water infiltration in SURF-TEMP to better predict the heat transfer between water and pavement material,
- Implement a fully implicit scheme in SURF-TEMP that includes the water-surface interface, to reduce model instabilities when water height is low and heat fluxes are high.

Bibliography

Anon., 2018. *CH2018 – Climate Scenarios for Switzerland, Technical Report,* Zurich: National Centre for Climate Services.

ASHRAE, 1993. *ASHRAE Handbook.* Atlanta: I-P Ed., American Society of Heating, Refrigerating and Air-Conditioning Engineers.

Azam, M. H. et al., 2018. A pavement-watering thermal model for SOLENE-microclimat: development and evaluation. *Urban Climate, 25,* pp. 22-36.

Azam, M. H. et al., 2018. A new urban soil model for SOLENE-microclimat: Review, sensitivity analysis and validation on a car park. *Urban climate, 24,* pp. 728-746.

Bentz, D. P., 2000. *A computer model to predict the surface temperature and time-of-wetness of concrete pavements and bridge decks,* Gaithersburg, MD, USA: National Institute of Standards and Technology.

Bergman, T. L., Incropera, F. P., DeWitt, D. P. & Lavine, A. S., 2011. *Fundamentals of heat and mass transfer.* s.l.:John Wiley & Sons..

Fowler, H. J. & Kilsby, C. G., 2003. Implications of changes in seasonal and annual extreme rainfall. *Geophysical Research Letters, 30(13).*

Hajat, S. & Kosatky, T., 2010. Heat-related mortality: a review and exploration of heterogeneity. *Journal of Epidemiology & Community Health, 64(9),* pp. 753-760.

Hendel, M., Colombert, M., Diab, Y. & Royon, L., 2015. An analysis of pavement heat flux to optimize the water efficiency of a pavement-watering method. *Applied thermal engineering, 78,* pp. 658-669.

Hendel, M. et al., 2016. Measuring the effects of urban heat island mitigation techniques in the field: Application to the case of pavement-watering in Paris.. *Urban Climate, 16,* pp. 43-58.

Herb, W. R., Janke, B. M. O. & Stefan, H. G., 2008. Ground surface temperature simulation for different land covers. *Journal of Hydrology, 356(3-4),* pp. 327-343.

Irvine Jr, T. & Duignan, M., 1985. Isobaric thermal expansion coefficients for water over large temperature and pressure ranges. *International communications in heat and mass transfer, 12(4),* pp. 465-478.

Johnson, G. & Geranios, N. K., 2021. *Northwest heat wave causes rolling blackouts in Washington state,* Washington state: Canada's National Observer.

King, A. D. & Karoly, D. J., 2017. Climate extremes in Europe at 1.5 and 2 degrees of global warming. *Environmental Research Letters, 12(11),* p. 114031.

Kusaka, H., Kondo, H., Kikegawa, Y. & Kimura, F., 2001. A simple single-layer urban canopy model for atmospheric models: Comparison with multi-layer and slab models.. *Boundary-layer meteorology, 101(3),* pp. 329-358.

Lafortezza, R., Carrus, G., Sanesi, G. & Davies, C., 2009. Benefits and well-being perceived by people visiting green spaces in periods of heat stress. *Urban forestry & urban greening, 8(2),* pp. 97-108.

McEvoy, D., Ahmed, I. & Mullett, J., 2012. The impact of the 2009 heat wave on Melbourne's critical infrastructure. *Local Environment, 17(8),* pp. 783-796.

Meehl, G. A. & Tebaldi, C., 2004. More intense, more frequent, and longer lasting heat waves in the. *Science, 305(5686),* pp. 994-997.

Min, J. & Tang, Y., 2015. Theoretical analysis of water film evaporation characteristics on an adiabatic solid wall. *International journal of refrigeration, 53,* pp. 55-61.

Min, S. K., Zhang, X., Zwiers, F. W. & Hegerl, G. C., 2011. Human contribution to more-intense precipitation extremes. *Nature 470,* p. 378–381 .

Moré, J., Garbow, B. & Hillstrom, K., 1980. *User guide for MINPACK-1,* Argonne, Illinois: Argonne National Laboratory.

Na, M. S., Shin, D. U. & Kim, Y. G., 2021. Study on the effect of timestep and thermography method for pavement watering technology. *Urban Climate, 39,* p. 100920.

Nayak, A. k., Hagishima, A. & Tanimoto, J., 2020. A simplified numerical model for evaporative cooling by water spray over roof surfaces. *Applied Thermal Engineering, 165,* p. 114514.

Pagliarini, G. & Rainieri, S., 2011. Dynamic thermal simulation of a glass-covered semi-outdoor space with roof evaporative cooling. *Energy and Buildings, 43(2-3),* pp. 592-598.

Palyvos, J. A., 2008. A survey of wind convection coefficient correlations for building envelope energy systems' modeling. *Applied thermal engineering, 28(8-9),* pp. 801-808.

Parison, S. et al., 2020. A lab experiment for optimizing the cooling efficiency and the watering rate of pavement-watering. *Urban Climate, 31,* p. 100543.

Parison, S., Hendel, M., Grados, A. & Royon, L., 2020. Analysis of the heat budget of standard, cool and watered pavements under lab heat-wave conditions.. *Energy and Buildings, 228.,* p. 110455.

Qin, Y. & Hiller, J. E., 2016. Water availability near the surface dominates the evaporation. *Construction and Building Materials, 111,* pp. 77-84.

Raimundo, A. M., Gaspar, A. R., Oliveira, A. V. M. & Quintela, D. A., 2014. Wind tunnel measurements and numerical simulations of water evaporation in forced convection airflow. *International journal of thermal sciences, 86,* pp. 28-40.

Reid, R., Prausnitz, J. & Poling, B., 1987. *The properties of gases and liquids.* s.l.:s.n.

Tang, R. & Etzion, Y., 2004. Comparative studies on the water evaporation rate from a wetted surface and that from a free water surface. *Building and Environment, 39(1),* pp. 77-86.

Tiwari, G. N., Kumar, A. & Sodha, M. S., 1982. A review—cooling by water evaporation over roof.. *Energy conversion and Management, 22(2),* pp. 143-153.

Wei, J. & He, J., 2013. Numerical simulation for analyzing the thermal improving effect of evaporative cooling urban surfaces on the urban built environment. *Applied thermal engineering, 51(1-2),* pp. 144-154.

Xia, Y. et al., 2018. Assessment of the economic impacts of heat waves: a case study of Nanjing, China. *Journal of Cleaner Production, 171,* pp. 811-819.

Appendix

Model 1.

$$Q_e = 0.622\frac{L_v h}{C_{p,air}P_0}T_w\left(\frac{P_{sat}(T_w)}{T_w} - \frac{RH \times P_{sat}(T_0)}{T_0}\right)$$

In the literature, Ts is used in the equation instead of Tw.

Model 2.

$$Q_e = 0.622\frac{L_v h}{C_{p,air}}\left(\frac{P_{sat}(T_w)}{P_0 - 0.378P_{sat}(T_w)} - \frac{RH \times P_{sat}(T_0)}{P_0 - RH \times 0.378P_{sat}(T_0)}\right)$$

In the literature, Ts is used in the equation instead of Tw.

Model 3.

$$Q_e = L_v h_m\left(\rho_{w,sat}(T_s) - \rho_w(T_s)\right)$$

The water vapor is assumed to be ideal gas.

Using the anology between heat and mass transfer,

$$\frac{h}{h_m} = \rho_{air}C_{p,air}Le^{\frac{2}{3}}$$

For air-water surface, the Lewis number can be assumed to be 1.

So,

$$Q_e = L_v h_m\left(\rho_{w,sat}(T_s) - \rho_w(T_s)\right) = \frac{L_v * h * 0.018}{8.314 * \rho_{air} * C_{p,air}} \times \left(\frac{P_{w,sat}(T_s)}{T_s} - \frac{RHP_{w,env}}{T_{env}}\right)$$

Model 4.

$$Q_e = 0.622\frac{L_v h}{C_{p,air}P_0}\frac{T_w + T_0}{2}\left(\frac{P_{sat}(T_w)}{T_w} - \frac{RH \times P_{sat}(T_0)}{T_0}\right)$$

Model 5.

$$Q_e = 10^{-9}L_v(37.17 + 32.19v)(P_{sat}(T_w) - RH \times P_{sat}(T_0))$$

Model 6.

$$Q_e = (0.2253 + 0.24644v)(P_{sat}(T_w) - RH \times P_{sat}(T_0))^{0.82}$$

Model 7.

$$Q_e = 0.013h(P_{sat}(T_w) - RH \times P_{sat}(T_0))$$

Model 8.

$$Q_e = 0.0015\rho_a L_v\left(v + (\theta_{v,w} - \theta_{v,0})^{0.33}\right) \times (\rho_{sat}(T_w) - RH\rho_{sat}(T_0))$$

$$\theta_{v,w} - \theta_{v,0} \cong T_w - T_0$$

$$\rho_{sat}(T_w) - RH\rho_{sat}(T_0) = \frac{0.018}{8.314}\left(\frac{P_{sat}(T_w)}{T_w} - \frac{RH \times P_{sat}(T_0)}{T_0}\right)$$

$$Q_e = 0.0015\rho_a L_v(v + (T_w - T_0)^{0.33}) \times \frac{0.018}{8.314}\left(\frac{P_{sat}(T_w)}{T_w} - \frac{RH \times P_{sat}(T_0)}{T_0}\right)$$

To reduce complexity of programming, temperature difference is used in our model instead of virtual temperature difference in the literature

Model 9.

$$Q_e = \frac{L_v}{r_a + r_s}(\rho_{air}(T_0) - \rho_{air,sat}(T_w))$$

$$r_a = \frac{K}{v}$$

For concrete surface, K is 50. Their experimental results show the regressed value of r_s to be 139 $\frac{s}{m}$ when the water content at the surface is 100%.

Model 10.

$$Q_e = k(w(T_w) - w(T_0))$$

$$w(T) = 0.0016T - 0.0204$$

$$w(T): humidity\ ratio\ of\ saturated\ moist\ air$$

$$k = \frac{h}{c_{p.air} Le^{\frac{2}{3}}}, Le = 0.85 \text{ for temperature between 20 and 40 °C}$$

$$Q_e = L_v \frac{h}{c_{p,a} L_e^{\frac{2}{3}}} (0.016 \times (T_w - 0.0204) - RH \times 0.016 \times (T_0 - 0.0204))$$

Temperature in the unit of °C. In the literature, the water temperature varies within the water film, whereas it's considered a constant value in out simulation.

Supplementary Figures

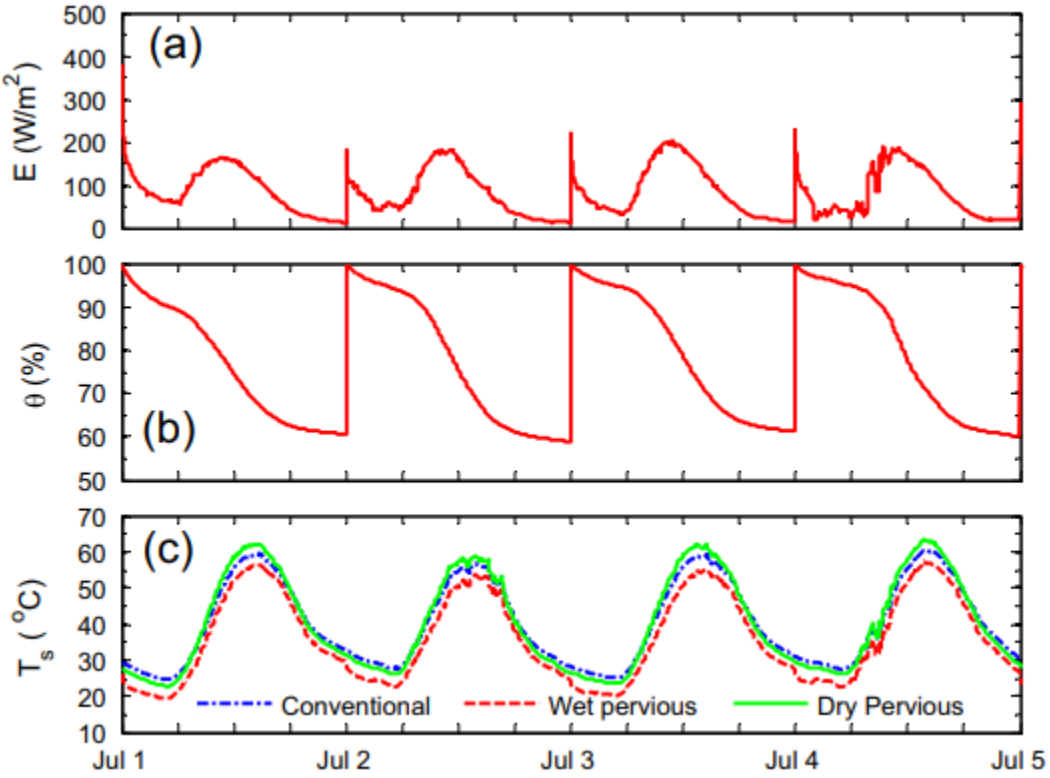

Figure 1. Evaporation rate from the pervious concrete surface versus time (Qin & Hiller, 2016)

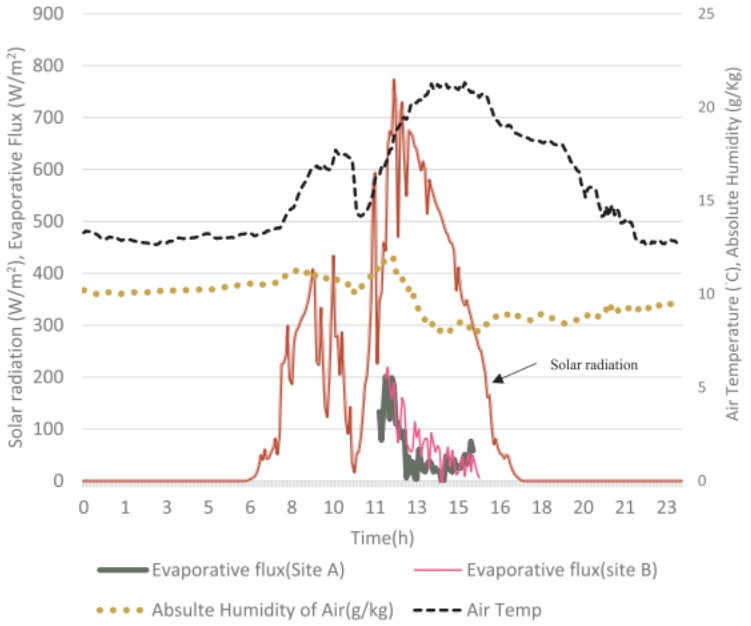

Figure 2. Field measurement of evaporative heat flux from (Nayak, et al., 2020). The precipitation happens around 11th hour)

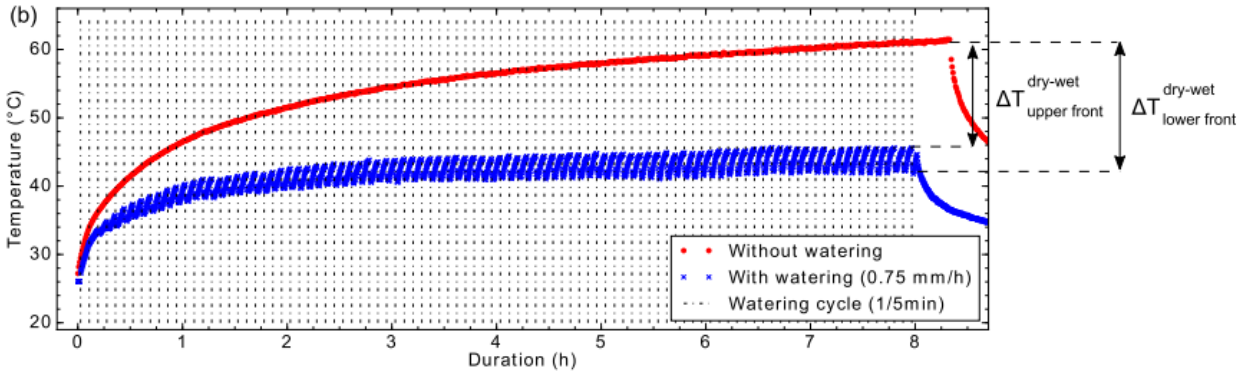

Figure 3. Pavement surface temperature variation with watering rate of 0.75 mm/hr (Parison, et al., 2020)